frontiers | Frontiers in Materials

REVIEW
published: 01 July 2022
doi: 10.3389/fmats.2022.906838

Recent Advances on Synthesis and Potential Applications of Carbon Quantum Dots

Vasanth Magesh, Ashok K. Sundramoorthy and Dhanraj Ganapathy*

Department of Prosthodontics and Material Science, Saveetha Dental College and Hospitals, Saveetha Institute of Medical and Technical Sciences, Chennai, India

Fluorescent carbon nanoparticles also termed as carbon quantum dots (CQDs) have attracted so much interest when compared to the traditional semiconductor quantum dots due to their applications in chemical sensing, biomedical imaging, nanotechnology, photovoltaics, light-emitting diodes (LEDs), and electrochemistry. Along with their optical features, CQDs have desired properties such as less toxicity, environmentally friendly nature, inexpensive, and simple preparation processes. In addition, CQDs can have their physical and chemical properties controlled by surface passivation and functionalization. This article provides an account of CQDs because of their distinct characteristics and considerable capacity in diverse applications. The article is categorized into various sections that highlight various synthesis methodologies of CQDs with their advantages/disadvantages and their potential applications in sensors, bio-imaging, drug delivery, solar cells, and supercapacitors. The different applications of CQDs can be demonstrated by controlled synthesis methods. We have also discussed gas sensing applications of CQDs briefly and provided a brief overview of osmotic power generation using CQDs for energy applications.

Keywords: carbon quantum dots, synthetic process, bio-medical applications, energy storage application, biosensors

OPEN ACCESS

Edited by:
Sandeep G. Surya, Dyson (United Kingdom), United Kingdom

Reviewed by:
Nazek El-Atab, King Abdullah University of Science and Technology, Saudi Arabia
Sanjit Manohar Majhi, United Arab Emirates University, United Arab Emirates

****Correspondence:***
Ashok K. Sundramoorthy
ashok.sundramoorthy@gmail.com

Specialty section:
This article was submitted to Carbon-Based Materials, a section of the journal Frontiers in Materials

Received: *29 March 2022*
Accepted: *23 May 2022*
Published: *01 July 2022*

Citation:
Magesh V, Sundramoorthy AK and Ganapathy D (2022) Recent Advances on Synthesis and Potential Applications of Carbon Quantum Dots. Front. Mater. 9:906838. doi: 10.3389/fmats.2022.906838

1 INTRODUCTION

From the last decade, carbon quantum dots (CQDs) have fascinated the interest of many global researchers. Specifically, carbon-based nanomaterials (CNMs) such as carbon nanotubes (CNTs) (Rao et al., 2018), graphene (Lin et al., 2018), nanodiamonds (Clancy et al., 2018), and fullerenes (Georgakilas et al., 2015) have gained more attention in the last few years. However, nanodiamond preparation and segregation are more challenging (Chauhan et al., 2020). CNTs, graphene, and fullerenes have low aqueous solubility, which makes them unable to produce brighter fluorescence in visible areas, and also have limited applications (Zhang et al., 2011). CQDs are a new family of CNMs with zero dimensions, having an average size of <10 nm (Jamaludin et al., 2019). CQDs are also known as carbon dots (CDs) in some cases. CQDs were first obtained in the preparative electrophoresis filtration of single-walled CNTs (Singh et al., 2018). Because of its benign, plentiful, and less cost, CQDs with intriguing features are considered a field of growing importance (Liu et al., 2020). Carbon is a dark-colored substance with a low water solubility and feeble fluorescence. Carbon-based quantum dots, also known as carbon nano-lights gathered much interest because of their high solubility as well as intense luminosity (Farshbaf et al., 2017). Similarly, carbon nano-dots (CNDs), graphene quantum dots (GQDs), and polymer dots (PDs) have

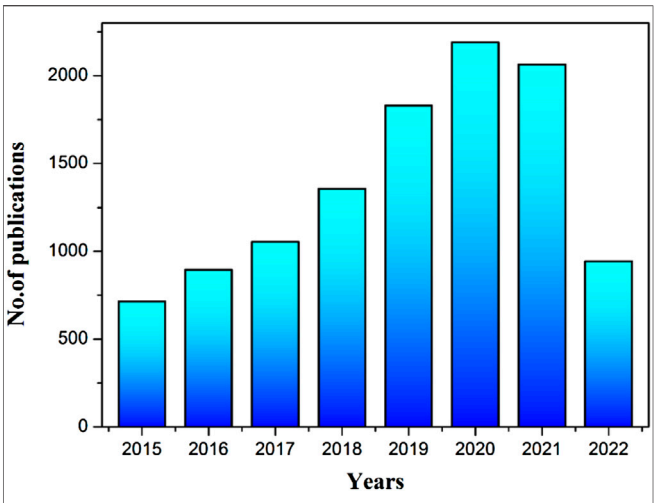

FIGURE 1 | The bar graph representing the increasing trend in the number of publications on "CQDs" in the period of 2015 to May 2022. These results were obtained from the Scopus database by using the keyword "carbon quantum dots" in the article title and abstract.

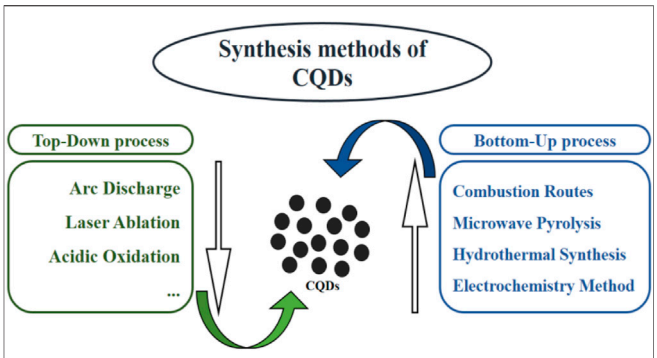

FIGURE 2 | Schematic diagram of various CQD synthesis methodologies.

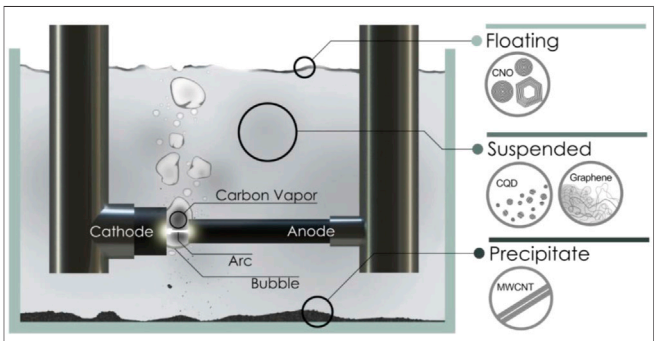

FIGURE 3 | Schematic representation of the submerged arc-discharge in water (SADW) method for production of CQDs. Reprinted with the permission from Chao-Mujica et al. (2021)).

also played a vital in this direction. GQDs, CNDs, and PDs are the same in appearance as well as photo-electrochemical characteristics, and although the chemical groups may differ in internal structure and morphology [11], they are the carbon-based skeleton of mono-dispersed spherical nanoparticles and a high concentration of oxygen groups present on their surface (Jeevanandam et al., 2018). For proper tuning of electrical structures of these materials to make photoluminescent, their size and chemical groups on the surface need to remain cautiously tuned (Smith and Nie, 2010). CQDs also have superior optical features of classic semiconductor quantum dots (SQDs) while compensating for the limitations of the traditional material when it comes to the environment, biohazard, and cytotoxicity. Great development is made in CQDs in terms of their production, characteristics, and functions in the last several years (Baker and Baker, 2010; Li et al., 2012; Shen et al., 2012). Photoluminescent carbon-based quantum dots outperform typical SQDs and organic dyes for their great solubility, elemental inactivity, and surface tenability as well as photobleaching defiance (Zheng et al., 2015).

Carbon-based quantum dots have prospective uses in imaging, drug delivery, and sensing of the biomolecules for their superior biological properties, such as minimal toxicity and good biocompatibility (Maiti et al., 2019). CQDs exhibited remarkable electronic capabilities as donors and acceptors of electrons, which cause chemi-luminescence and electrochemical luminescence that permitted them to be used in many applications such as in optronics, catalysis, and sensing (Chen et al., 2020). In addition, CQDs have shown excellent properties such as eco-friendly, harmless, greater water solubility, quantum size-effect property, bio-compatible, and cost-effective. The CQDs can be synthesized by using different facile techniques. However, there are still some problems in the performance and efficiency of the CQDs. The CQDs itself may not fulfil all the requirements. Therefore, additional functional groups are introduced on the CQDs surface. The surface modified CQDs are not superior compared to SQDs. Hence, further research is required to improve the properties of CQDs in order to match its performance as similar to SQDs (Lim et al., 2015).

To highlight the importance of CQD-based research, we have used the Scopus database to find out the total number of articles published up to date using the keyword "carbon quantum dots" in article title and abstracts. As shown in **Figure 1**, it is very obvious that the number of research papers on CQDs is keeping on increasing every year. This review article provides latest developments on CQDs' synthesis, their distinct characteristics, and various potential applications. The review article is categorized into various sections that include various CQD synthesis methodologies and their potential applications in sensors, bio-imaging, drug delivery, solar cells, and supercapacitors.

2 SYNTHESIS METHODOLOGIES OF CQDS

Synthesis methods of CQD are categorized into two types: (i) top-down and (ii) bottom-up techniques (Carbonaro et al., 2019). Physical or chemical methods are used in the top-down approach

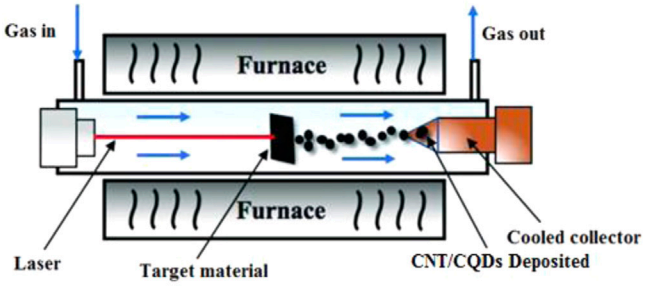

FIGURE 4 | Diagram depicting the progression of CNT/CQDs formation using the laser ablation process. This image was modified and reprinted with the permission from Zan Lu et al. (2019).

to destroy or disperse the bulk carbon source into small-sized CQDs (**Figure 2**). The top-down methodologies are known as arc-discharge, laser ablation, and acidic oxidation (Pillar-Little et al., 2018). The bottom-up approach involves a series of chemical reactions that polymerize and carbonize small molecules into CQDs. The bottom-up synthesis methods are microwave pyrolysis, combustion routes, the electrochemical method, and hydrothermal/solvothermal synthesis (Singh et al., 2018) (El-Shabasy et al., 2021).

2.1 Top-Down Approaches

2.1.1 Arc-Discharge

This method involves reorganizing carbon molecules during breakdown from bulk carbon sources powered by gas plasma produced in a sealed reactor in an anodic electrode (**Figure 3**) (Arora and Sharma, 2014). Under the electric current, the temperature in the reactor can achieve 4,000 K, resulting in plasma with huge energy. Carbon vapor assembles in the cathode to generate CQDs. During the synthesis of single-walled carbon nanotubes (SWCNTs) by the arc discharge technique, a team of researchers from the United States generated three types of carbon nanoparticles with comparative molecular masses and photo-luminescence (Dey et al., 2014).

The fluorescence of the as-prepared CQDs can be orange, blue-green, or yellow at 365 nm. The carboxyl group (hydrophilic) was introduced on the surface of CQDs by using HNO_3. Because of the different scales and very low yield of carbon particles generated during the arc-discharge method, the CQDs obtained by this approach showed strong water solubility with a large particle size of around 18 nm in general. Furthermore, nanoparticles obtained from arc-discharge may also contain a number of complicated components that were challenging to filter and remove (Zuo et al., 2016). Chao-Mujica et al. synthesized CQDs in water using a submerged arc-discharge process. The obtained CQDs have exhibited a quantum yield of 16% and emitted two consistent bands in the spectrum of 320–340 nm (band A) and 400–410 nm (band B) with excitation wavelengths of 275 nm (band A) and 285 nm (band B), respectively. These CQDs were utilized as a fluorescent biomarker for *in-vitro* investigations on L929 murine fibroblasts in a cell culture (Chao-Mujica et al., 2021). This approach can provide CQDs that can be used in bio-imaging applications. This kind of CQD showed a low quantum yield (QY) and limited particle size scalability. However, it had shown a good photoluminescence (PL) property.

2.1.2 Laser Ablation Method

This method illuminates the objective's surface with a great-energy laser pulse. As a result, it enters a thermodynamic state with extremely high pressure (75 KPa) and temperature (> 900°C), which rapidly warms up and condenses to a plasma state where vapor crystallizes for the formation of carbon nanomaterials (Hu et al., 2011). A simple method for producing CQDs is by irradiating a carbon precursor dispersed in various conventional organic solvents with a laser (**Figure 4**). The synthesized carbon nanoparticles were aggregated with varied sizes and showed no observable PL. The sample was then treated with a dilute HNO_3 solution and refluxed for 12 h before being reacted by polyethylene glycol (PEG) (Zuo et al., 2016). The CQDs were discovered to have visible and tunable photoluminescence (Li et al., 2011). The surface condition of CQDs can be adjusted by using the appropriate organic solvent to vary the PL properties of the created CQDs and passivated CQDs having high PL with a diameter of around 5 nm. Laser ablation is a useful technique for making CQDs with a restricted size distribution, high water solubility, and fluorescence (Hu et al., 2009). The fluorescence QYs of CQDs were ranged from around 4%–10% when excited at 400 nm (Desmond et al., 2021).

Ren et al. reported the pulsed laser ablation approach that was used to create N-doped micro-pore CQDs (NM-CQDs). The NM-CQDs had a QY of 32.4 percent and a fluorescence lifespan of 6.56 ns. Because of the stable and strong PL emission, these CQDs were employed for cellular staining and imaging, which displayed good internalization in many cells (Ren et al., 2019). Cui et al. reported the dual beam laser ablation method to create CQDs from low-cost carbon fabrics. It has been used for cell bio-imaging and demonstrated 35.4 percent QY. As-synthesized CQDs by laser ablation was applied in biomedical imaging. Generally, CQDs emit more PL (depending on the solvent and precursor) and this approach produces more PL emissions (Cui et al., 2020). An enormous number of raw materials are required to make CQDs, and the particle sizes could not be controlled, resulting in low QY, which are the disadvantages of this method. It is worth mentioning that this method is rapid and effective and the surface state of CQDs is tunable.

2.1.3 Acidic Oxidation

Exfoliating and disintegrating bulk carbon into nanoparticles while concurrently inserting hydrophilic functional groups on the surface such as hydroxyl or carboxyl groups has been a common method (Shen and Xia, 2014). The synthesis of hetero-atom-doped CQDs in a large scale using acidic oxidation and hydrothermal reduction was reported in 2014. To begin, a combination of HNO_3, H_2SO_4, and $NaClO_3$ was used to oxidize carbon nanoparticles obtained from Chinese ink (Yang et al., 2014). The oxidized CQDs were then hydrothermally

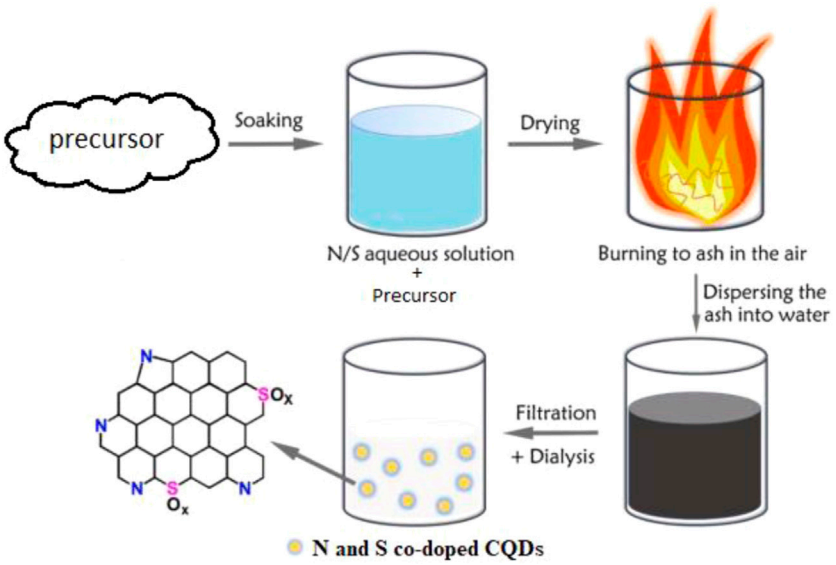

FIGURE 5 | Schematic illustration of the preparation of N/S co-doped CQDs. This was adapted and modified with the permission from Cheng et al. (2019).

reacted with nitrogen, sulfur, and selenium sources. Respectively, di-methyl formamide (DMF), sodium hydro-sulfide (NaHS), and sodium selenide (NaHSe) have been used as precursors. In comparison to pure CQDs, the produced N-CQDs, S-CQDs, and Se-CQDs have exhibited adjustable longer fluorescence life span, better PL performance, and good quantum yield (QY). The heavily doped hetero-atoms can change the PL characteristics that are favorably connected to the electro-negativities of N, S, and Se, according to the findings. When utilized as electrocatalysts, the electronic framework of the associated CQDs would be changed by the active hetero-atoms on the surface, which provided good electrocatalytic activity (Hassan and Saleh, 2021). However, heavily doped CQDs have the potential to interact with group 3 to 12 metal ions in the periodic table, and N-CQDs, S-CQDs, and Se-CQDs might have the ability to attract a few additional metal ions, such as Fe^{3+}, Co^{2+}, and Ni^{2+}, to generate single-atom catalysts (SAC) (Jiang et al., 2015). Feng et al. synthesized CQDs from coke by using this method, which showed 9.2% of QY (Feng and Zhang, 2019). Similarly, Iannazzo et al. prepared GQDs from multi-walled carbon nanotubes (MWNT) through the acidic oxidation technique for targeted HIV treatment, medication, and delivery. For the goal of targeting, reverse transcriptase inhibitors (RTIs) were changed on the surface of GQDs (Iannazzo et al., 2018). Tang et al. reported an acidic oxidation process that was used to make GQDs from graphene oxide (GO). The obtained GQDs had shown peroxidase-like catalytic activity and used to detect H_2O_2 with a detection limit of 87 nM. CQDs are also employed to prepare electrochemical sensors and drug delivery applications after it was produced by the acidic oxidation technique (Tang et al., 2016). The acidic oxidation method is simple and effective to produce CQDs on large scale. However, in this method, some strong oxidizers may be used, which could cause burning or explosion, and the post processing is also very complicated.

2.2 Bottom-Up Approach

2.2.1 Combustion Route

Combustion pathway is a simple technique with easy scaling up, precisely controlled design of starting molecules, cheap, and environmentally friendly process, so it received great attention in improving the bottom-up strategies for CQD production (Varma et al., 2016). Combustion methodology has been proposed for the CQDs' synthesis, which got quickly adopted by numerous researchers (Xu et al., 2018). For example, fluorescent graphene quantum dots (GQDs) were produced by combusting citric acid and then functionalized with carboxyl groups via acetic acid moiety conjugation at high temperatures. GQDs in a homogeneous size of 8.5 nm with abundant carboxyl groups on the surface were produced (Li S. et al., 2017). The N/S-co-doped CQDs were efficiently fabricated by a one-step combustion treatment of cellulose-based bio-waste willow catkin (Salix gracilistyla) (**Figure 5**) (Cheng et al., 2019). The synthesized CQDs have a homogeneous size distribution and a large number of carboxyl groups present in the structure. This method of production is simple and easy to scale up. The combustion method produced small polycyclic aromatic hydrocarbons (PAHs) that are an existential hazard (Desmond et al., 2021).

Xiang et al. reported the thermal pyrolysis (combustion) process to make multicolor emissive CDs from citric acid and urea. The photoluminescence QY of blue, green, and red emissions reaches as 52.6%, 35.1%, and 12.9%, respectively, on the CDs. The CDs can also be uniformly disseminated in epoxy resins and produced as clear CDs/epoxy composites for devices that output different colors and white light (Miao et al., 2018). This method is simple, large-scale synthesis is possible, and CDs exhibited high QY and good PL intensity. The CQDs obtained from this method could be used for bio-imaging and optoelectronic applications.

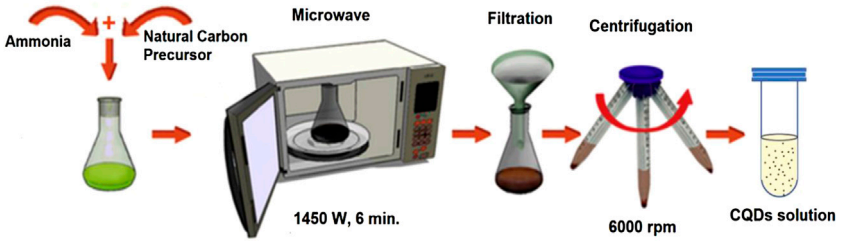

FIGURE 6 | Synthesis procedure for microwave-assisted pyrolysis for CQDs. This was adapted and modified with the permission from Monte-Filho et al. (2019).

2.2.2 Microwave Pyrolysis

Microwave pyrolysis is one of the most well-known bottom-up techniques due to its simplicity and commercialization viability. CQDs were produced with the help of microwave irradiation using a modified commercial microwave (**Figure 6**) (Başoğlu et al., 2020). Microwave irradiation causes polar molecules in the solvent to interact with opposing electric and magnetic fields, resulting in atomic level heating. This method is effective because the high frequency energy created by the electromagnetic radiation is directly applied to the reactions with no physical interaction or medium. This method resulted in a quicker reaction with a higher selective yield and energy. As a result, when compared to other existing heating methods, this method offered rapid synthesis, eco-friendly, an energy and time saving method, minimal impurity, size and temperature regulation with enhanced safety, good reproducibility, and excellent control over reaction conditions that all resulted in impressive CQDs' synthesis (Tungare et al., 2020). A simple microwave pyrolysis method was reported for the production of CQDs by mixing poly(ethylene-glycol) and a saccharide in water, which formed a clear solution that later was heated it in a microwave (Zhu et al., 2009).

The PL characteristics of the produced CQDs were excitation-dependent. As-obtained CQDs with oxygen-containing groups could serve as metal ion coordination sites in the development of carbon-based electrocatalysts. Zhu et al. reported the QY of synthesized CQDs as 82.7%. After a dialysis filtration, it drops to 45.1%, and after a phase transfer filtration, it drops to 57.5% (Zhu et al., 2021). The highest QY observed was 61.3% for N-S-CQDs synthesized by the microwave-assisted method (Wang et al., 2015). Nakano et al. reported N-CQDs for H_2O_2 detection, which was synthesized from citric acid using a one-spot microwave aided technique (Nakano et al., 2018). Arsalani et al. reported the microwave pyrolysis technique to synthesize polyethylene glycol linked fluorescent carbon dots (PEG-CDs) from gelatin for drug delivery application. Due to its enhanced nuclear delivery *in vitro*, the PEG-CDs act as a nano-carrier for an anticancer drug of methotrexate (MTX), which demonstrated as a better antitumor efficacy than free MTX, and it resulted in extremely effective tumor growth inhibition and enhanced targeted cancer therapy (Arsalani et al., 2019). Shejale et al. also reported the microwave pyrolysis method to produce N-CQDs. These NCQDs were used in the dye sensitized solar cell (DSSC)/quantum dot sensitized solar cell (QDSSC) construction to boost the device performance. The usage of NCQDs as a co-photoactive layer resulted in a high photo-conversion efficiency of 8.75% and a photocurrent density of 18.13 mA/cm^2 under one solar irradiation. As a co-sensitizer and sensitizer, the achieved power conversion efficiency was from 55% to 99%, which was better than NCQDs (Shejale et al., 2021). This method produced CQDs with good physiochemical and optical features, including wide spectrum absorption, high charge carrier extraction, rapid charge carrier transportation, and tunable emission. Although it is a convenient one-stop and environmentally friendly method, the size of the CQDs cannot be controlled. This method is also rapid, scalable, cost-effective, and eco-friendly to produce CQDs.

2.2.3 Electrochemical Methods

The electrochemical approach is a straightforward and convenient method of preparation that could be performed at ambient temperature and pressure (Ahirwar et al., 2017). The electrochemical approach for CQD synthesis is broadly reported because of its ease in altering the particle dimension and their PL performance. Electrochemical carbonization of sodium citrate and urea in deionized (DI) water produced blue-emission CQDs (size ~2.4 nm) that might be used as a highly subtle detector for Hg^{2+} in the discarded water (Hou et al., 2015). As a result, the idea of combining CQD synthesis and electrocatalyst fabrication in a single-pot electrochemical process seems attractive. As shown in **Figure 7**, CQDs were produced using a three-electrode setup with a working electrode (WE) as a graphite electrode, a counter electrode (CE) as a platinum foil or Pt wire, and a reference electrode (RE) as an Ag/AgCl electrode. As an electrolyte, alkaline alcohol (e.g., 0.1 M NaOH/EtOH) was utilized. The colorless CQD dispersion was achieved by applying a stable potential of 5 V to the graphite electrode (working electrode) for 3 h in a nitrogen (N) environment (Liu et al., 2016). The electrolyte remained transparent throughout the electrochemical oxidation process for CQD production, and the graphite electrode surface did not enlarge significantly. This occurrence was differed from other publication, which reported brown CQD dispersal and an enlarged electrode when graphite rods or other carbon materials were used as working electrodes (Devi et al., 2018).

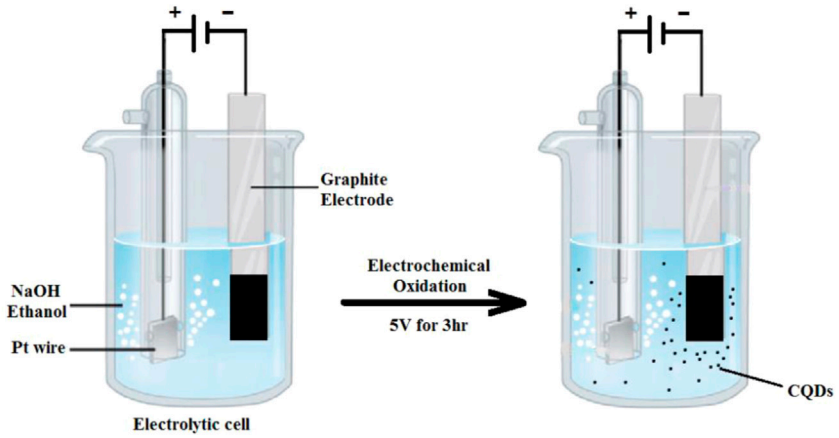

FIGURE 7 | Schematic illustration for CQD generation via an electrochemical oxidation of the graphite electrode in alkaline alcohols.

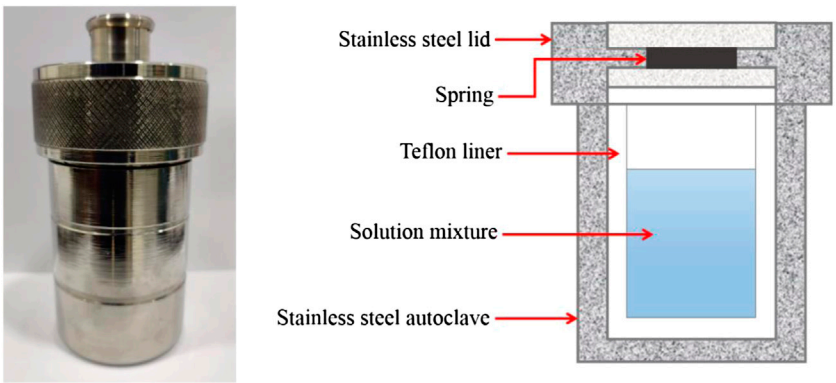

FIGURE 8 | Schematic representation of the Teflon-lined stainless-steel hydrothermal autoclave.

It can be observed that the EC approach for CQD synthesis has used alkaline alcohol as an electrolyte. This method can be considered as an environmentally friendly, low-cost method and highly repeatable (Liu et al., 2016). Tian et al. reported the QY of exfoliated CQDs as 5.6%. Sun et al. also synthesized Fe-N-CQDs, which showed 7.5% of QY by utilizing the electrochemical method which is lower than that of other methods (Tian et al., 2020; Sun et al., 2021). Niu et al. (2017) reported the photoluminescence and electroluminescence applications of N-GQDs that were synthesized from different ammonia solutions via an electrochemical technique. These NCQDs have shown a wide range of applications, including efficient cell imaging, fiber staining, and Fe^{3+} detection. Ramila et al. also reported the synthesis of CQDs from graphite sources for sensing applications. A CQD-based sensor was used to detect dopamine with the LOD of 99 nM (Devi et al., 2018). Electrochemically synthesized CQDs are employed in bio-imaging and sensor applications. This method is a sustainable and environmentally beneficial method. However, it has poor size control. The CQDs obtained by the electrochemical method showed high level stability, and the size distribution is uniform. The pre-treatment of raw material and purification of CQDs are time-taking processes and also difficult to estimate the concentration of the CQDs.

2.2.4 Hydrothermal/Solvothermal Methods

A hydrothermal process is a bottom-up method that involves an easy system set-up as well as the particles formed in uniform size with a great quantum yield. The hydrothermal method is one of the most often utilized procedures in CQDs' synthesis (Thambiraj and Shankaran, 2016). To make the reaction precursor, organic compounds of small size are suspended in water or an organic solvent. Then, it transferred into the stainless steel autoclave lined with Teflon, which is commonly used in the laboratory for the hydrothermal method (**Figure 8**) (He et al., 2018). At a relatively high temperature, organic molecules merged to produce carbon seeding cores, which grew into CQDs with sizes less than 10 nm (Azam et al., 2021).

The highest QY of CQDs was around 80% which was nearly equal to fluorescent dyes. CQDs were made with a high yield utilizing carbon and nitrogen sources (citric acid and ethylenediamine) in a hydrothermal procedure. As-synthesized

CQDs were used to prepare biosensors for sensing of Fe^{3+} in living cells (Pu et al., 2019). Full-color CQDs with controlled photo-luminescence at many different wavelengths were created by adjusting the quantity of graphitic nitrogen in hydrothermal conditions. Furthermore, biomolecules with abundant carbon and nitrogen could be employed for proper tuning of interior architectures of CQDs during hydrothermal condensation (Lu S. et al., 2019). This technique is a potential strategy for designing and fabricating novel electrocatalysts with customizable doping composition and electronic architectures because of its simple synthetic procedure and variable hetero-atom doping. Atchudan et al. reported CQDs made from banana peels using a hydrothermal technique for bio-imaging, and they displayed 20% QY (Atchudan et al., 2021b). Arumugam et al. synthesized CQDs from broccoli using a hydrothermal process and used it to fabricate sensors. The CQDs can detect Ag^{+} with the LOD of 0.5 μM (Arumugam and Kim, 2018). Mahani et al. also synthesized CQDs by hydrothermal carbonization of citric acid and then modified with transferrin (TF) to enhance water solubility and association with specific cell receptors. The drug (doxorubicin) was loaded onto a TF-CQD carrier for delivery to breast cancer cells (MCF-7) (Mahani et al., 2021). Similarly, Sahoo et al. reported hydrothermal fabrication of NiS-CQDs from lime juice for supercapacitor applications with a specific capacity of 880 Fg^{-1} at a current density of 2 Ag^{-1}. With a particle size of 1.3 nm, the compound remained unchanged up to 2000 charge-discharge cycles (Sahoo et al., 2018). Huang et al. synthesized CdS-CQDs by a hydrothermal technique using cotton fiber and urea, which was later used in quantum dot sensitized solar cells (QDSCs) with an average size of 2.97 ± 0.4 nm. CdS-CQD-derived QDSCs have exhibited a power conversion efficiency of 0.606%. This was 40.9% higher than QDSCs based on CdS (0.430%) (Huang et al., 2020a).

When we compare the benefits of all the methods used for the production of CQDs, the hydrothermal method is a simple one and yielded CQDs with high QY, controllable particle size, and no need of expensive chemicals. CQDs obtained from hydrothermal was also employed in bio-imaging, drug administration, sensor development, solar cells, and supercapacitors. The hydrothermal method is cost effective, eco-friendly, and non-toxic. This method may yield CQDs with various sizes and low QY.

3 PROPERTIES OF CQDS

3.1 UV–Visible Absorption

The UV–visible absorption (UV–vis) spectrum could reveal the information of emission as well as excitation states of the material. In CQDs, the UV–vis absorption produced from various precursors in various solvents is visibly different. CQDs have a variety of configurations, but they all absorb UV light in the same way. Rather than providing specific instances, we will simply list some frequent UV–visible absorption phenomena. In the UV range of 260–320 nm, the more absorption peaks may usually be seen clearly (Azam et al., 2021). The absorption spectrum of CQDs can be observed in the wavelength region of 220–270 nm. It is clear that electrons can move to the C=N bonds from the π-orbit. Electronic transition from C–O or C=O bonds to the π^{*} orbital is responsible for the absorption spectrum in the 280–350 nm range (**Figure 9**). The electronic transition of the polar functional groups of CQDs is ascribed to the absorption spectral region of 350–600 nm, demonstrating that surface chemical components may lead to absorbance in the UV–visible ranges (Kang et al., 2020). According to several studies, the absorption band of CQDs red-shifted when surface functional groups are treated or their sizes are adjusted. Even certain exceptional CQDs exhibit longer absorption spectra of 600–800 nm, which are attributed to aromatic ring-containing architectures. The N-CQDs unlike the previously stated CQDs had a high excitonic absorption spectrum due to their quantum size. The discrepancies in absorption spectra of CQDs reflect their differences in the structures and distinct hybridization or compositions to a certain extent (Holá et al., 2017).

3.2 Photoluminescence

In the past few years, the study into PL is one of the intriguing aspects of CQDs, and it has exploded with applications in photocatalysis and other fields. The wavelength of PL emission is larger than the wavelength of excitation, as is the case with Stokes-type emission (Chu et al., 2019). There were also numerous reports in the literature on the observations of PL emissions in CQDs, which are being attributed to a variety of sources. A detailed look at the spectroscopic characteristics of the emissions, as well as the structural properties of the underlying materials, showed that the majority of the detected PL emissions may be divided into two groups. The first is related to band-gap transition associated with conjugated π-domains, while the second one is due to more complex causes that are more or less linked to deficiencies in graphene structures. The production or inducement of the π-domains is frequently predicated on the exploitation of flaws in graphene sheets; therefore, the two aspects may be intertwined in many circumstances (Cao et al., 2013). Several researches have explored the correlation between the excitation wavelength (λex) and PL emission of CQDs. The ex-dependent emission of fluorescent CQDs with the surface modification of polyethylene glycol (PEG-1500N) or propionylethyleneimine-coethyleneimine (PPEI-EI) is clearly visible, as shown in **Figure 10** (Sun et al., 2006). This behavior was further validated by another study, which found that CQDs synthesized by one-step thermal treatment of 4-aminoantipyrine, which emit the ex-dependent PL emission from 525 to 660 nm with excitation wavelengths ranging from 425 to 625 nm (Wang R. et al., 2017).

Apart from the excitation wavelength, the PL emission of CQDs is also examined in relation to their size manipulation. CQDs with the sizes of around 1.2–3.8 nm were synthesized using a one-step alkali-assisted electrochemical technique. Optical views of CQDs with four different sizes, exposed in white (natural-light lamp) and UV-light (365 nm), are shown in **Figure 11**. The PL spectra for blue-, green-, yellow-, and red-emitting CQDs are red, black, green, and blue lines, respectively. A thorough investigation revealed that the PL characteristics fluctuate dramatically with the size of CQDs, indicating that

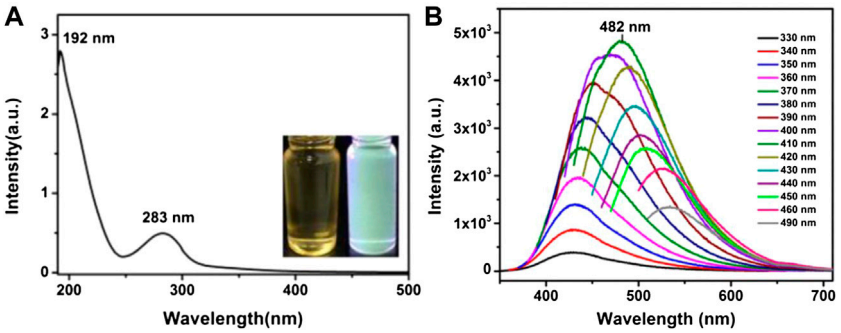

FIGURE 9 | (A) UV–Vis absorption spectra of CQDs, inset: optical images under daylight (left) and UV light (right). **(B)** PL spectra of CQDs at different excitation wavelengths. Reprinted with permission from He et al. (2018).

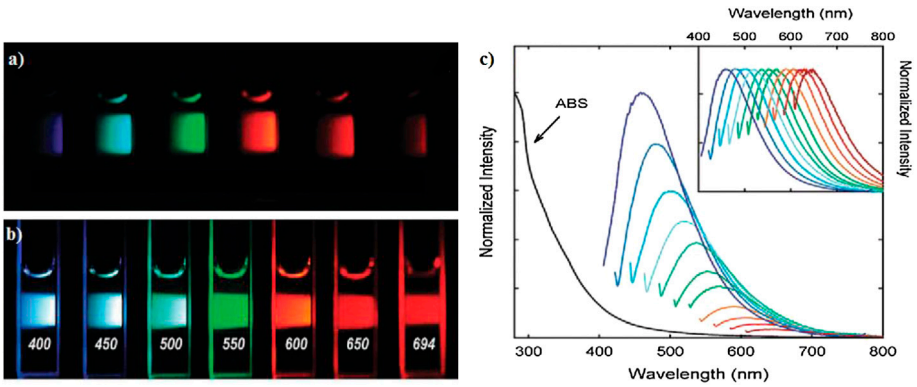

FIGURE 10 | Aqueous solution of the PEG-CQDs: **(A)** excited at 400 nm and photographed through bandpass filters of different wavelengths as indicated and **(B)** excited at the indicated wavelengths and photographed directly. **(C)** Absorbance (ABS) and luminescence emission spectra (with progressively longer excitation wavelengths from 400 nm on the left in 20 nm increment) of propionylethyleneimine-co-ethyleneimine (PPEI-EI) CQDs in an aqueous solution. The emission spectral intensities are normalized to quantum yields (inset: normalized to spectral peaks). Reprinted with permission from Sun et al. (2006).

the HOMO-LUMO gap is highly dependent on the particle size (Zhu et al., 2015). The band-gap decreases significantly as the particle size increases, and the gap energy in the visible wavelength range can be acquired from particles with diameters ranging from 1.4 to 2.2 nm, which also agrees well with the visible spectrum emission of CQDs with diameters less than 3 nm. As a result, they indicated that the potent emission of CQDs is caused by a quantum-sized graphite structure rather than the carbon–oxygen surface. CQDs obtained from different alkyl-gallates with various sizes exhibited a similar steady-state of PL spectra, indicating that CQD PL emission is size-independent (Hola et al., 2014).

3.3 Up-Conversion Photoluminescence

The certain CQDs emit UCPL emissions in addition to normal photoluminescence (PL) emission (Zong et al., 2011). In contradiction to regular PL, UCPL emission has a lesser energy emission spectrum than the excitation spectra, i.e., the excitation wavelength is longer than the emission wavelength. This is especially appealing for *in-vivo* bio-imaging, as bio-imaging at longer wavelengths particularly in the NIR region is typically favored due to increased photoelectron tissue penetration and lower background self-fluorescence. When activated by an 800 nm femto-second pulsed laser (FPL), the authors have reported that their CQDs produce visible light, implying that they had up-conversion capabilities (Zheng et al., 2015). Following that, numerous additional groups discovered up-conversion fluorescence emissions (UCFE) from CQDs made using fundamentally different synthetic techniques (Wang et al., 2012). In addition to regular down-conversion, the fluorescence intensity of CQDs produced by immediately heated ascorbic acid solution at 90°C has exceptional UCFE features (Jia et al., 2012). Green illumination with a peak wavelength of 540 nm was released from their CQDs after stimulation in the near-infrared region of 800–1,000 nm. The multiphoton excitation mechanism is a key component that, most likely caused the UCFE.

The multiphoton excitation is insufficient to compensate for the UCFE characteristics of CQDs due to the nearly constant band-gap energy of 1.1 eV between both the excitation and

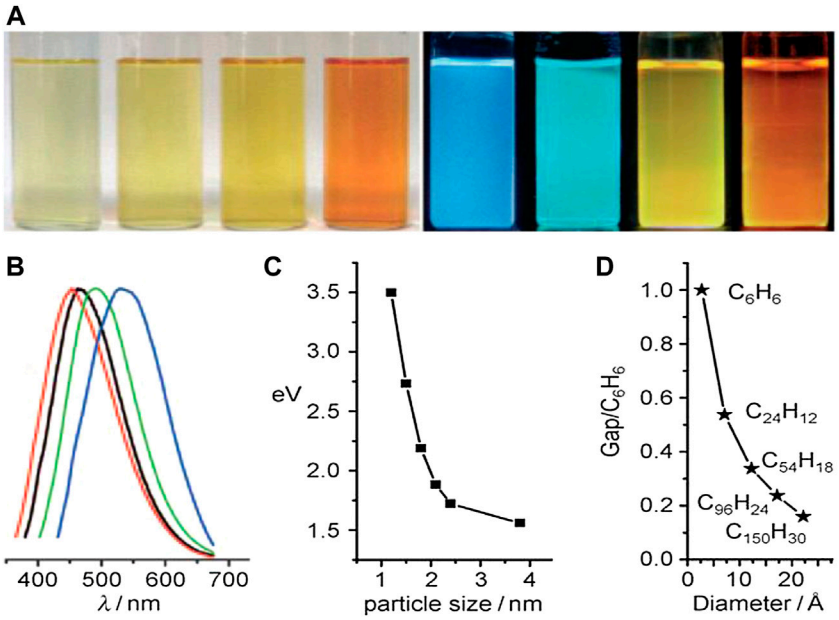

FIGURE 11 | Size effect of CQDs. **(A)** Typical sized CQDs optical images illuminated under white (left; daylight lamp) and UV light (right; 365 nm); **(B)** PL spectra of typical sized CQDs: the red, black, green, and blue lines are the PL spectra for blue-, green-, yellow-, and red-emission CQDs, respectively; **(C)** relationship between the CQD size and the PL properties; and **(D)** HOMO–LUMO gap dependence on the size of the CQDs. Reprinted with permission from (Li et al., 2010).

emission photons (Zuo et al., 2016). They speculated that such UCFE is caused by electrons relaxing from a greater energy level of the π-orbital (LUMO) to the σ-orbital, since when a greater number of lower energy photons excite the electrons in the π-orbital, a few electrons will inevitably migrate to the LUMO. The electrons in the σ-orbits can be excited as well, but they only release down-conversion light. A few of the observed UCFE, on the other side, are artefact's arising from typical down-conversion emissions stimulated by the leaky components from the spectro-fluorometer of mono-chromator second diffraction. The leaky component can be repaired by simply introducing a long-pass filter into the excitation channel. As a result, significant caution must be used when evaluating CQD fluorescence emissions, and more information is needed to understand up-conversion CQDs (Wen et al., 2014).

3.4 Photo-Induced Electron Transfer

In solutions, the CQDs either will be electron acceptors or electron donors that can be quenched effectively, indicating that photo-induced CQDs are also both greater electron donors and acceptors. Despite the fact that this photo-induced electron transfer property of CQDs has been widely reported, a direct demonstration and understanding of the photo-induced charge dissociation in CQDs has yet to be achieved (Roy et al., 2015). Through redox reactions, certain indirect analytical proof was gained. Photoluminescence decay experiments of CQDs using the recognized electron acceptor 2, 4-dinitrotoluene (−0.9 V vs. NHE) and electron donor N,N-diethylaniline (DEA, 0.88 V vs. NHE) revealed this PIET characteristic (Zhang et al., 2012). CQDs' significant PIET property opens up new possibilities for redox processes such as light energy conversion as well as associated applications. CQDs in compound photocatalysts can efficiently capture photo-generated electrons from semiconductors, resulting in improved photo-induced electron and hole separation efficiency (Xia et al., 2016). In addition, the photo-excited CQDs' redox active nature was established in the metal ion reduction in an aqueous solution. The production and depositing of the noble metal (silver, gold, or platinum) on the surface of CQDs are caused by the treatment of CQD aqueous solution with a noble metal (silver, gold, or platinum) salt. Hence, the noble metal is electron-affinitive, and it absorbs electrons from the attached CQDs, disturbing radiative recombination's once more, resulting in the exceptionally effective static quenching of fluorescence emissions exhibited (Xu et al., 2012).

3.5 Electroluminescence

As semiconductor nanomaterials are well-known for exhibiting electroluminescence (EL), it is no surprise that CQDs have sparked interest in EL research that could be useful in electrochemical domains (Xu et al., 2018). The emission color of CQD-based light emitting diodes (LEDs) can be adjusted by the driving current. Under various working voltages, color switchable EL from the identical CQDs ranging from blue to white was observed. The researchers developed two theories based on the band-gap emitters of a conjoined p domain and the edge effect generated by some other surface irregularities to better explain the luminescence process of CQDs (Sk et al., 2014). The quantum-confinement effect of p-conjugated electrons in the sp2 atomic structure determines the PL properties of CQD fluorescence emission from the conjugated p domain, which can be changed by its scale, edge orientation, and morphology.

Surface flaws such as sp2 and sp3 hybridized carbon as well as other surface irregularities of CQDs cause fluorescence emission, and even fluorescence emission and peak positioning are connected to this defect (Wang et al., 2014).

3.6 Chemiluminescence

The CL characteristics of CQDs are first found, when the CQDs co-existed with oxidants such as potassium permanganate ($KMnO_4$) and cerium (IV). Oxidants like $KMnO_4$ and cerium (IV) can introduce holes into CQDs, according to electron paramagnetic resonance (EPR) (Lin et al., 2012). This process boosts the abundance of holes in CQDs and speeds up electron–hole annihilation, leading to CL emission and energy release. Furthermore, the CL intensity was influenced by CQD concentrations within a particular range. The optimal temperature of electron dispersion in CQDs was also discovered to have a favorable impact on the CL when the temperature was raised. The fact that the CL characteristics can be designed by modifying their surface groups is intriguing for this system (Teng et al., 2014). In a highly alkaline solution, a novel CL phenomenon was noticed for the CQDs as prepared (NaOH or KOH). In a solution of NaOH, the CQDs showed high electron donor capacity towards dissolved oxygen, forming the superoxide anion radical (O_2^-). The greatest electron-donating potential of CQDs was directly demonstrated by these findings. The CL performance in highly alkaline solutions has been attributed to the recombination rate of the injected electrons by "chemical reduction" of the CQDs and thermally stimulated produced holes. The CL of CQDs opens up new possibilities for their use in reductive substance analysis. CQDs' dual activity as an electron donor and acceptor has enormous potential in optometry and catalysis (Zhao et al., 2013).

3.7 Biological Properties

Developing vibrant CQD bio-probes with better stability has made significant development. However, with further utilization in live cells, tissues, and animals, biocompatibility of the functionalized CQDs remains a crucial challenge. Over the last several years, systematic cytotoxicity tests have been performed on both surface modified and unmodified CQDs. The arc-discharge of graphite rods yielded CQDs, which were subsequently refluxed in HNO_3 for 12 h for cytotoxicity testing. Up to a rather higher concentration of 0.4 mg/ml, raw CQDs appeared to be harmless to cells. Luminescent CQDs made by electrochemically treating graphite were also tested in a cytotoxicity assay employing a human kidney cell line, and the dots had no effect on the cell viability. Besides, a soot-based method for the production of CQDs with an average diameter of 26 nm was used (Hong et al., 2015). The CQDs showed little cytotoxicity at the doses required for fluorescence cell imaging, according to the outcome of cell viability experiments. In cytotoxicity tests, the cytotoxicity of the CQD surface modified with functional groups such as PPEI-EI, PEG, PEI, BPEI [branched poly-(ethylenimine)], and PAA [poly(acrylic acid) was assessed (Cao et al., 2007; Yang et al., 2009; Dong et al., 2012; Wang et al., 2011)]. The PEGylated CQDs are non-cytotoxic at dosages far greater than those required for cell imaging and applications in all possible configurations. Furthermore, mice treated with CQDs passivated with PEG1500N for toxicity testing for up to 28 days, also with results indicating no major adverse effects *in vivo*. Furthermore, the PPEI-EI passivated CQDs were mainly harmless to the cells under a considerably large threshold of carbon core-equivalent PPEI-EI concentration, according to the data (Ding et al., 2014). As per the MTT [3-(4,5-dimethylthiazol-2-yl)-2,5-diphenyltetrazolium bromide] experiment, even at quite high doses, a PEI-free sample was evidently harmless to HT-29 cells. PEI-modified CQDs were more toxic to cells than PPEI-EI-modified CQDs. Because PEI is the homo-polymer equivalent to PPEI-EI with an ultimate EI fraction of 100 percent, the more ethylenimine (EI) units inside the PEI may be related with lesser concentration thresholds for CQDs to become cytotoxic. Even at modest concentrations ($50\ mg\ ml^{-1}$), free PAA in a water insoluble solution was considered to be toxic to cells. At a certain CQD core comparable concentration level, the PAA-modified CQDs were comparable to free PAA and are both toxic to the cells after a 24-h exposure and less so after a 4-h exposure. PEG and PPEI-EI, for example, are suitable for CQDs modified for *in-vivo* imaging and biosensing because they have minimal cytotoxicity even at higher concentrations. If the concentrations were kept lower enough and the exposure time is kept short enough, molecules with higher cytotoxicity, such as BPEI and PAA, can still be employed to modified CQDs used *in vivo* (Namdari et al., 2017).

3.8 Catalytic Properties

CQDs have been widely used in the photocatalytic field to improve catalyst activity due to their high photocatalytic activity. For example, visible-light responsive CQDs produced from pear juice used for effective methylene blue (MB) degradation (Das et al., 2019). CQDs' excellent light absorbance and electron transport were credited with their higher photocatalytic activity. In less than 2.1 h, the deterioration ratio of MB had reached 95 percent. By loading CQDs made from orange peel waste onto ZnO, C-dots/ZnO composite based catalyst was prepared (Prasannan and Imae, 2013). The C-dots/ZnO composite catalyst has shown a greater photocatalytic performance than the ZnO catalyst (Prasannan and Imae, 2013). The excited electrons from ZnO are transported to CQDs in this manner, preventing the electron–hole pairs from recombining. Due to the interaction between ZnO and water, hydroxyl radicals are formed. Likewise, the interaction of electrons on CQDs with oxygen produced superoxide ions. The produced superoxide ions can be used to destroy azo dye. CQDs made from lemon peel waste are immobilized on TiO_2, resulting in a CQDs/TiO_2 composite catalyst (Tyagi et al., 2016). MB dye was degraded using the CQDs/TiO_2 catalyst that was obtained. These findings showed that CQDs are important in the realm of photocatalysis. In addition, the CQDs/TiO_2 composite was effective for methyl orange decomposition (Deng et al., 2021). The presence of H^+ and $^{\bullet}OH$ in visible light was related to the deterioration ability.

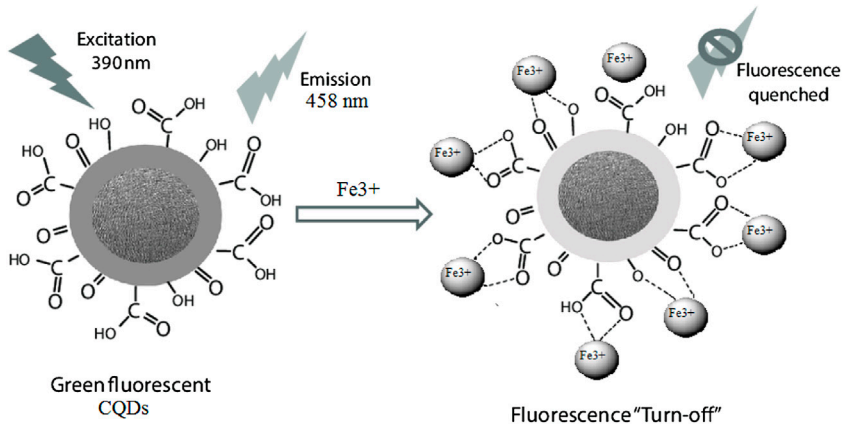

FIGURE 12 | Surface passivated green fluorescence CQDs [positively charged ions (Fe^{3+}) or attracted by the negatively charged surface of the CQDs for sensing confirmation by fluorescence quenching mechanism].

4 POTENTIAL APPLICATIONS OF CQDS

CQDs have recently attracted a lot of attention as a potential opponent to standard SQDs because of their nontoxicity, chemical stability, high optical absorptivity, and ease of synthesis (Drummen, 2010). CQDs could be a viable substitute for harmful metal-based quantum dots. Applications of CQDs in various fields such as energy, chemical sensing, optronics, and biological application have been demonstrated (Namdari et al., 2017). CQDs are also used in a variety of energy-related industries (including supercapacitors and solar cells) (Li X. et al., 2015) and in biological applications such as bio-imaging, bio-sensing, and drug delivery (Devi et al., 2019). It has also been used for chemical sensing of heavy metal ions (Matea et al., 2017). CQDs has also been used in sensors, photocatalysts, and optical devices such as light-emitting diodes due to their superior optical and electronic capabilities (LED) (Soley, 2017). In the below section, we have discussed recent applications of CQDs in sensors, bio-imaging, drug delivery, solar cells, and supercapacitors.

4.1 Sensors

CQDs have emerged in recent years for their use in the preparation of sensor systems with lower limit of detection (LOD), even up to pico- or femto-molar ranges. Advantages of CQDs are facile production, low cost synthesis procedures, simple functionalization routes, outstanding brightness, high QY, chemically stable, and minimal toxicity (Zhou C. et al., 2021; Zhang et al., 2020). When the sample contains a metal ion (like Fe^{3+}), CQD sensors work by quenching or blocking the CQD's absorption spectrum (Arumugham et al., 2020). The charge transfer mechanism could be the cause of the fluorescence emission attenuation. **Figure 12** shows the function of the Fe^{3+} ion fluorescence sensor, which is on the emission quenching of CQDs. Static quenching, dynamic quenching, inner filter effect (IFE), photo-induced electron transfer (PET), and fluorescence resonance energy transfer (FRET) are all the different quenching mechanisms of the CQDs (Zu et al., 2017). Static quenching is when a quencher interacts with the CQDs, resulting in the development of a non-fluorescent ground-state complex. In static-quenching, the development of the ground-state complex may change the emission spectra of CQDs (Tang et al., 2021). Herein, an increase in temperature can damage the durability of the ground-state complex, reducing the static-quenching effect. In dynamic-quenching, the excited position of CQDs comes back to their ground state as a result of energy transfer among the CQDs and quencher. In comparison to static-quenching, dynamic-quenching has definitely no effect on the optical absorbance of CQDs and only disturbs the excited position of the CQDs (Zu et al., 2017). In addition, the appearance of the quencher may alter the lifespan of CQDs. When it comes to dynamic quenching, a rise in the temperature can help to strengthen the dynamic quenching effect. When energy is shifted from a higher-energy donor to lower-energy acceptor, the contact of two fluorescent molecules divided by a range of typically 10 nm leads to magnification of the acceptor fluorescence at the loss of the donor fluorescence or quenching. The role of FRET of quantum dots (QD) in analyte sensing is schematically represented. At first, the existence of a quencher reduces the QD's emission.

The presence of a quencher in close proximity suppresses the QD's emission at first. The QD emission can be recovered, especially when the quenching dye interacts competitively with the target molecule in the vicinity of the analyte (Oh et al., 2005). The IFE is caused by the absorber in a sensor system absorbing the photon to do excitation and/or emission of light. To construct the IFE-based detection system, an absorbent and a fluorescent must be present in the system. The absorber's (particles) absorption spectrum overlaps with the fluorescence emission and/or excitation spectrum in the IFE model. As a result, the absorber can control the emission of fluorescence (fluoro-particles) (Molaei, 2020). Furthermore, absorber's absorption should be precise and responsive to the system's analyte concentration. Sensors based on CQDs have been used to detect a variety of species, including metal ions, acids, water contaminants, drugs, and other compounds. CQD-based sensors

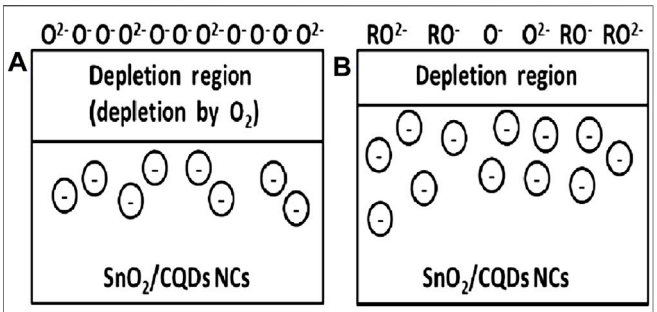

FIGURE 13 | (A) Oxygen extract electrons from metal oxide, thereby decreasing conductivity, and **(B)** when reducing agent (R) is present, electrons are injected into the oxide again and thus increasing conductivity. Reprinted with permission from Prajapati et al. (2021).

appear to be interesting with more possibilities for high-performance, yet precise sensors in a wide range of applications.

4.2 CQDs for Gas Sensors

Gas sensor devices are critically needed to monitor air pollution and maintain human health. Advancements in the field of small semiconductor structures could overhaul the notion of traditional gas sensors in this area. The distinctive electrical and optical capabilities of semiconductor materials are due to the containment of charge transfer in one or more spatial dimensions (Nikolic et al., 2020). Quantum dots (QD), which contain electron–hole pairs in all three dimensions, provided new perspectives into material characteristics. QD based chemical sensor research has been among the most quickly growing topics in modern sensing technology. QDs' structures have demonstrated significant sensing capability, showing that they are becoming a new group of materials for use in chemi-resistive systems. Therefore, detection systems are only now beginning to incorporate QD-based frameworks (Zhang and Wang, 2012). The results of the experiments indicate that more research is needed to fully comprehend the impact of synthesis techniques and added materials on QD sensing properties. Furthermore, the materials' sensitivity and selectivity should be examined on the basis of the band-gap alterations in QDs when the diameter is adjusted.

On the semiconductor surface, the gas adsorptions are classified into two types: physical adsorption (physisorption) and chemical adsorption (chemisorption). The van der Waals forces drive physisorption, which is a weakly dipolar attraction between solid materials and gas molecules. In physisorption, the heat produced is below 6 kcal/mol. In chemisorption, a strong contact between solids and gas molecules resulted in charge transport between the solid surface and gaseous species. In chemisorption, the heat produced is larger than 15 kcal/mol. As a result of the temperature rises, the physisorption process decreases and chemisorption increases. At high temperatures, physisorption might turn into chemisorption (Chang, 2016). Oxygen is the most essential part of air. As a result, the contact of semiconducting materials with oxygen is critical for detecting other gases in the atmosphere. Generally, gas sensors can work in the range of room-temperature (RT) to 500°C (Galstyan, 2017). The ions adsorbed (ionosorbed) oxygen in molecular (O_2^-) and atomic (O^-) forms can trap the surface electrons during these temperatures. At working temperatures less than 150°C, the O_2^- ions predominate on the sensing element, whereas at higher temperature than 150°C, the O^- atomic forms predominate. As a result, the ionosorbed oxygen species take electrons from the n-type semiconductor's conduction band, forming a depletion region and a Schottky barrier (qVs) at the grain boundaries, as shown in **Figure 13**. Wang et al. reported silica aerogel surface modification with highly fluorescent CQDs, which was used to detect NO_2 gas in a precise and sensitive way. BPEI-CQDs (branched polyethylenimine-capped quantum dots) have 40% higher than QY. The fluorescence intensity of the CQD modified aerogels may be quenched by NO_2 gas in a sensitivity and selectivity manner, and there is a decent linear relationship between the fluorescence quenching ratio and NO_2 quantity (Wang et al., 2013).

Yu et al. reported the fabrication of the ZnO/CQD composite using hydrothermally synthesized ZnO and CQDs. Herein, CQDs are doped into ZnO by mechanical grinding and mixing, which was used to prevent the surface properties of CQDs from being damaged throughout high-temperature reactions. The ZnO has a wurtzite hexagonal structure with a flower-like microsphere shape, which allowed for larger surface areas for adsorbed gases. In comparison to ZnO nanoparticles, the ZnO/CQD composite displayed a greater gas sensitivity reaction to nitric oxide (NO) gas. The ZnO/CQD combination demonstrated a high NO sensitivity (gas-sensing response R_g/R_0 is 238 for 100 ppm NO at 100°C) and selectivity. The ZnO/CQD composite exhibited a LOD of 100 ppb for NO and a response and recovery time of 34 and 36 s, respectively (Yu et al., 2020). Arunragsa et al. reported hydroxyl-modified GQDs (OH-GQDs) onto the inter-digitated nickel electrode to create a different RT gas sensor. The OH-GQDs were made by utilizing a bottom-up strategy involving pyrene hydrothermal treatment. The results demonstrated that the RT OH-GQD gas sensor has good selectivity and sensitivity as well as a rapid reaction to ammonia (NH_3) at concentrations ranging from 10 to 500 ppm (Arunragsa et al., 2020). Prajapati et al. have used the grape juice to make SnO_2/CQDs by the hydrothermal technique. The SnO_2/CQDs based nanocomposite was used as the sensing elements in the sensor. The applications of CQDs on the gas-sensing sensitivities and selectivity were examined. At 275°C, the SnO_2/CQD nanocomposite showed better performance for sensing of carbon monoxide with high-sensitivity (Prajapati et al., 2021).

4.3 Photoluminescence Sensors

The fluorescent sensors can detect a variety of metal ions as well as other chemical species (Tammina et al., 2019; Wu et al., 2019). Generally known detection methods of metal ions/chemical species are atomic absorption spectroscopy (AAS) or inductively coupled plasma mass spectrometry (ICP-MS), which are costly and inflexible, and cannot be employed rapidly on the field because of their obstinacy, size, and cost. Due to the relatively low cost, simple handling, and great selectivity and sensitivity, fluorescence-dependent sensors are a

TABLE 1 | The CQDs synthesized from various precursors for sensor applications and measured parameters (LOD, QY, and heavy metal detection).

Product	Precursor	Synthesis method	To detect	LOD	Quantum yield	Reference
FeN_x-CQDs	Carbon cloth electrode of Fe-N-C	Electrochemical oxidation	Cu^{2+}	59 nM	7.2%	Sun et al. (2021)
CQDs	Diammonium hydrogen citrate & urea	Solid-state reaction	Fe^{3+}	19 μM	46.40%	Khan et al. (2017)
CDs	Plectranthus amboinicus	Hydrothermal method	Ag^{+}	10 nM	—	Dineshkumar et al. (2019)
CQDs	Waste polyolefins	Microwave pyrolysis	Cu^{2+}	6.33 nM	4.84%	Kumari et al. (2018)
N-CQDs	Isoleucine and citric acid	Hydrothermal method	Fe^{3+}	0–60 μM	—	Jiang et al. (2015)
N & S-CQDs	Citric acid and urea	Microwave-assisted method	Hg^{2+}	2 μM	25%	Libo Li et al. (2015)
KN-CDs	*Actinidia deliciosa*	Hydrothermal-carbonization	Fe^{3+}	0.85–0.95 μM	—	Atchudan et al. (2021a)
CQDs	Hyper-branched polyethyleneimine (hPEI) and 2,4-dihydroxybenzoic acid (DA)	Hydrothermal method	Cu^{2+}	193 nM	—	Yang et al. (2021)
CQDs	*Borassus flabellifer*	Thermal pyrolysis	Fe^{3+}	10 nM	—	Murugan and Sundramoorthy, (2018)
O-CQDs	*Oxalis corniculata*	Hydrothermal method	Fe^{3+}	0.73 μM	—	Atchudan et al. (2021c)
CQDs	*Eleusine coracana*	Thermal pyrolysis	Cu^{2+}	10 nM	—	Murugan et al. (2019)
CQDs	Ammonium citrate and citric acid + 1,10-phenanthroline	Microwave pyrolysis	Hg^{2+}, Cu^{2+}, and Fe^{3+}	3, 0.5, and 30 nM	—	Dejie Li et al. (2020)
CQDs	Jinhua bergamot	Hydrothermal method	Fe^{3+}	0.075 μM	50.78%	Yu et al. (2015)

Footnotes: FeN_x-CQDs (mono-atomic iron anchored nitrogen-doped CQDs), N-CQDs (nitrogen doped CQDs), N & S-CQDs (nitrogen and sulphur co-doped CQDs), KN-CDs (CDs from kiwi fruit peel), and O-CQDs (CQDs from Oxalis corniculata).

better solution for detection of metal ions. The free CQDs in aqueous solutions have a fluorescence feature. The fluorescence emission intensity may alter or disappear due to the prevalence of a quencher inside the solution due to energy or charge exchange between the CQDs and quencher (Molaei, 2019).

Low LOD values are one of the key benefits of CQD-based fluorescence sensors. If the LOD value is low, the sensor is ultra-sensitive. While these conditions were repeated, ions such as Fe^{2+}, Hg^{2+}, Pb^{2+}, Cd^{2+}, Mn^{2+}, and Fe^{3+} were added to the solution. CQDs behaved differently in the presence of various ions, which was because the synthesized CQDs had a high selectivity for Fe^{3+} ions in solution (Liu et al., 2022). **Table 1** shows the comparison of facile synthesis methods reported for CQDs from various organic and inorganic precursors for selective heavy metal detection. The doped and un-doped CQDs had shown good QY (25%–50.78%) as well as lowest LOD (19 μM–10 nM).

4.3.1 Chemiluminescence Sensor

Chemiluminescence (CL) is a type of electromagnetic radiation created by a chemical reaction involving two reagents, wherein light is released as a stimulated intermediary or product relaxes to its ground state (Chen et al., 2016; Amjadi et al., 2017). Because of its simplicity and high sensitivity, the CL is used in analytical chemistry. Luminol, potassium permanganate, peroxalate, and lucigenin are the most often used and investigated CL reagents in analytical chemistry. However, the traditional reagents have a number of disadvantages, such as high cost, toxic effects, and low sensitivity (Hallaj et al., 2017). In terms of instrumental needs for CL measurement, the CL is simple because here the excitation UV–visible spectra or a spectral resolving apparatus is not required. Light is in fact emitted as a by-product of the chemical process. This method is especially sensitive since it measures a minimal quantity of emitted illumination in CL as in lack of noise. Nevertheless, in CL, most LODs are determined by reagent purity rather than detector (sensor) sensitivity, which accounts for lower LOD levels. CQDs can enhance CL systems in a number of ways, including the following: a) focusing the excited CL emitter, which results in increased CL emission; b) in the reaction, the CQDs can act as a catalyst; and c) CQDs have the power to cause the CL response to occur. The removal of electron and hole-injected CQDs may cause CL emission. The CQDs act as a catalyst for CL of luminol without the use of any extra oxidant (Zong et al., 2018). This behavior could be caused by the reaction between CQDs and luminol, as well as the formation of an active transition complex, which could speed up the electron exchange process in the luminol-dissolved oxygen CL reaction. Modifying the surface states of the dots was found to impact both CL emission and CQD catalytic activity. CQDs' catalytic activity can be improved by inducing the carboxyl and carbonyl group on their surfaces (Chu et al., 2019). CQDs have the ability to boost H_2O_2–HSO_3's ultra-weak CL intensity by up to 60 times. This was achieved by forming excited position CQDs (CQDs*), which are produced by annihilating positively and negatively charged CQDs via electron transfer. CQDs produced negatively and positively charged surfaces by reacting with the •OH radical, $•SO^{3-}$, $SO^{4•-}$, and $•O^{2-}$ anionic radicals formed by the interaction of H_2O_2 and HSO_3^-. In addition to dopamine, Cr(VI), and adrenaline in water, CL sensors were utilized to detect 4-nitrophenol, Cu^{2+}, Fe^{2+}, bisphenol A, indomethacin, hydrogen peroxide, and other compounds (Shah et al., 2016).

4.3.2 Electro-Chemiluminescence Sensor

Several nanostructures including GQDs, PDs, nanocrystals, and inorganic nanocomposites have been employed as luminophores in various ECL systems in recent studies (Qin et al., 2019). Furthermore, these kinds of nanomaterials including heavy

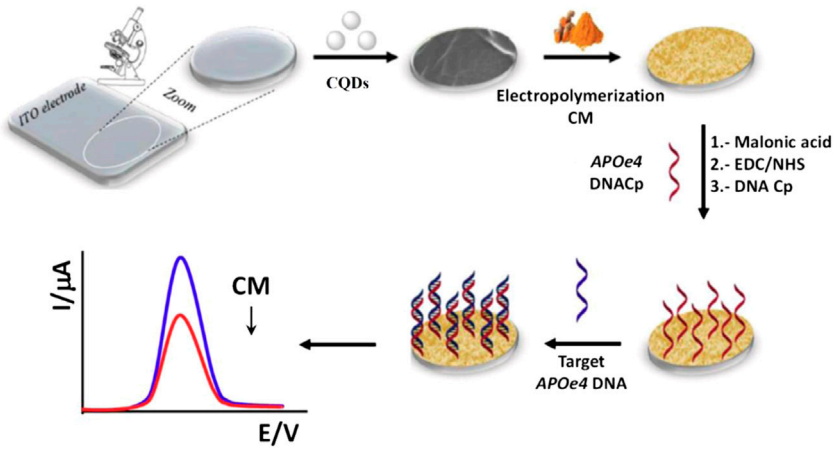

FIGURE 14 | Schematic representation of the electrochemical DNA biosensor. Reprinted with the permission from (Campuzano et al., 2019).

metals comprising QDs such as CdS, CdSe, CdTe, and CdTe/ZnS are poisonous and have low biocompatibility and lower sensitivity in some circumstances. CQDs are an emerging nanostructure that has been used in ECL systems (Xu et al., 2014). When compared to semiconductor QDs, CQDs with exceptional optical characteristics such as PL and CL make good ECL luminophores because of their simple synthesis procedure, chemical inertness, easy functionalization, lesser toxicity, and simple labelling. By targeting APOe4 DNA, a double fluorescence and electrochemical DNA sensor based on an indium-tin oxide (ITO) electrode modified with curcumin, (CM)/GQDs, has been shown to detect Alzheimer's and arterial coronary disorders. On the GQDs-ITO surface, the electro-polymerization of the CM molecule was carried out with double fluorescent and electrochemical characteristics. A malonic acid spacer was employed to covalently immobilize an amino-substituted DNA probe using 1-ethyl-3-(3-dimethylaminopropyl) carbodiimide/N-hydroxy succinimide (EDC/NHS) chemistry, as shown in **Figure 14** (Campuzano et al., 2019).

The creation of excited position CQDs* at the electrodes by an electron-transfer mechanism between positively charged CQDs$^{\bullet+}$ and negatively charged CQDs$^{\bullet-}$ is suggested to Stokes as the source of ECL emission by CQDs (Dong et al., 2013). To achieve the increased ECL activity, CQDs can be utilized as luminophores in the double luminophores ECL system. The CQDs were employed in an ECL system with a perylenetetracarboxylic acid (PTCA) luminophore and a carcinoembryonic antigen immunosensor. With a LOD of 0.00026 fg ml^{-1}, the immunosensor demonstrated exceptional sensitivity. The existence of $S_2O_8^{2-}$ as a co-reactant combines with minimal species of CQDs$^{\bullet-}$ and PTCA$^{\bullet-}$ to produce an excited position of CQDs* and PTCA*, resulted in the development of the excited position of CQDs (CQDs*) and PTCA (PTCA*). Light is emitted when the excited position of CQDs* and PTCA* is created. The surface states have an impact on the ECL emission of CQDs (Chen et al., 2020). CQDs produced a strong ECL emission when the voltage in the ECL system was cycled with Pt sheets as WE and CE and Ag/AgCl as the RE. Mechanical milling produced CQDs with numerous surface states. There was no ECL indication in the absence of the CQDs. The ECL response is greatly increased when $K_2S_2O_8$ is added as a hole donor. The CQDs revealed dual-wavelength ECL peaks due to their synthesis process, which creates two types of surface states on their surface (Han et al., 2015). The ECL peaks are more right shifted in visible spectra by rising the emission wavelength than the PL spectra, implying that the ECL signal is more reliant on surface conditions than the PL signal. CQDs can be immobilized using graphene, a two-dimensional carbon sheet. Which can magnify the ECL signal of the CQDs due to their huge surface area, excellent chemical stability, superior electrical property, good mechanical stability, and high electro-catalytic activity. The CQDs were immobilized on graphene in an ECL sensor to detect chlorinated phenols in water samples. An ECL signal is produced by the correlation of the CQD's excited position (CQDs*) and the analyte with the help of $S_2O_8^{2-}$ (as a co-reactant). The inclusion of graphene sheets aids in the creation of CQDs$^{\bullet-}$ and $SO_4^{\bullet-}$, resulting in a high CQDs^{*+} production yield. In the cathodic ECL process, the exceptional capacity of graphene sheets in electron movement leads to electron transfer from the electrode to CQDs and $S_2O_8^{2-}$. As a result, CQDs$^{\bullet-}$ and $SO_4^{\bullet-}$ generation will be facilitated. The ECL signal is a 48-fold amplification as a result of the multistage amplification. This sensor has a LOD of 1.0×10^{-12} M in the range of 1.0×10^{-12} to 1.0×10^{-8} M. Different species have been detected using ECL systems with the use of CQDs (Yang et al., 2013).

4.4 Bio-Imaging

Bio-imaging refers to a non-invasive technique for visualizing the biological system in actual time. Bio-imaging attempts to interfere with living processes even less than possible. Furthermore, it is frequently used to obtain information about the studied specimens in the 3-D structure from outside, i.e., without medical intervention. Bio-imaging is a larger sense, referring to methods for imaging living cells that have been maintained for study. Bio-imaging encompasses the study of subcellular framework and whole cells as well as tissues and multicellular

TABLE 2 | Synthesis of CQDs from various organic and inorganic precursors for bio-imaging applications and their noticeable parameters of Ex/Em wavelengths, average particle size, and QY.

Product	Precursor	Synthesis method	Excitation/ Emission wavelength	Average particle size	Quantum yield	Tested	Reference
CQDs	Banana peel	Hydrothermal	365/520 nm	5 nm	20%	Nematode	Atchudan et al. (2021b)
CQDs	Walnut shells	Carbonization	360/450 nm	3.4 nm	—	MC_3T_3 cells	Cheng et al. (2017)
CQDs	Wheat straw and bamboo residues	Hydrothermal	365/520 nm	6 nm	13%	Smmc-7721 tumour cells	Caoxing Huang et al. (2019)
CQDs	Citric acid and ethanediamine	Hydrothermal	375/535 nm	<10 nm	—	HeLa cells	Xue et al. (2019)
CQDs	Citric acid and p-phenylenediamine	Hydrothermal	360/496 nm	3.6 nm	8.55%	HeLa cells	Huo et al. (2021)
CQDs	*Eleocharis dulcis*	Hydrothermal	380/458 nm	10 nm	—	Fe^{3+} ions	Bao et al. (2018)
CQDs	Tetraphenylporphyrin	Hydrothermal	360/480 nm	2.7 nm	15.20%	HeLa cells	Wu et al. (2017)
CQDs	Vitamin B1	Hydrothermal	367/420 nm	3.2 nm	4.40%	Fe^{3+} ions	Wu et al. (2018)
N-CDs	L-arginine and D-glucose	Hydrothermal	365/450 nm	—	21%	A549 cells	Xu et al. (2021)
P,N-CQDs	Cyanobacteria, H_3PO_4 and $C_2H_8N_2$	Hydrothermal	370/445 nm	—	8.13%	PC12 cells	Wang et al. (2021)
N,P-CQDs	Ganoderma lucidum	Hydrothermal	332/410 nm	3.12 nm	11.41%	U2OS and HT29	Tu et al. (2020)
N,S,P-CDs	Thiamine pyrophosphate	Hydrothermal	340/440 nm	2 nm	32%	SK-MEL28	Nasrin et al. (2020)

Footnotes: N-CDs (nitrogen doped Carbon Dots), PN-CQDs (phosphorus-nitrogen doped CQDs), NP-CQDs (nitrogen, phosphorus c-doped CQDs), and NSP-CQDs (nitrogen, sulfur and phosphorus multi-doped CQDs).

organisms. CQDs have been identified as desirable candidates for bio-imaging due to a greater tunable photoluminescence (PL), lesser toxicity, hydrophilic nature, and great opto-chemical stability under UV irradiation. Although, most of the CQDs effectively generate blue emission with a short excitation spectra, which severely limits bio-imaging (Wang X. et al., 2019; Marković et al., 2020). Several studies have shown that the hetero-atom doped CQDs have extended wavelengths and multicolor fluorescent, making them suitable for longer period and actual time cell imaging as well as *in vivo* bio-imaging. The use of cell images demonstrated that N-CQDs with excellent biocompatible might tag with PC12 cells. In comparison to single hetero-doped CQDs, dual hetero-atoms of nitrogen, phosphorus, or boron co-doped with CQDs display excellent biocompatibility and high QY. The o-phenylenediamine (OPD) and boric acid (BA) used for the synthesis of yellow fluorescent N,B-CQDs by the microwave-assisted hydrothermal method. 50 g/ml of N,B-CQDs is treated with HeLa cells to produce the fluorescence image (Liu et al., 2018).

HeLa cells emitted bright yellow fluorescence, principally in the cytoplasm post-treatment with N, B-CQDs under illumination at a specific wavelength of 405 nm, and there was no major difference in the cellular structures or survival rate. When N, P-CDs concentrations reached 1,000 g/ml, no harmful effects were observed in the human bone cancer cell (U2OS) or human colon cancer cell (HT29) (Martynenko et al., 2017). On the other hand, multi-doping has received less attention because of the complicated methods and reaction conditions required. When compared to (dual-atom) co-doped CQDs, the (three atom) tri-doped CQDs have rich functional species on the surface which incorporated more excited position, among these are the excited electrons in CQDs, go through the inter-state conversion as well as radiative recombination, resulting in a variety of fluorescence emissions at specific wavelengths. Because of its similar size to carbon, N plays a vital function in electrical modification. The introduction of the N-dopant was created a special surface pattern that can facilitate intense radiation recombination. Through a collaborative effect, the inclusion of sulphur improves the effect of N atom-doped CQDs. However, adding a third species decreases the size of CQDs and enhances fluorescence QY and efficiency dramatically, just like F-doping in the carbon moieties improves ORR catalysis. Doped CQDs have various advantages in sensing and bioimaging because of their unique property. The function of specific elemental dopants in generating multicolor emissions in CQDs, on the other hand, has yet to be investigated. **Table 2** shows QY, Ex/Em wavelength of un-doped, single atom doped, dual atoms doped and three atoms doped CQDs. These results pointed to a promising future as a suitable cell imaging vehicle for *in-vivo* imaging.

4.5 Drug Delivery

Chemotherapy is commonly used to treat cancer and other disorders, although it lacks precision and is associated with toxicity and multi-drug resistance. As a result, targeted medication administration is chosen as a way for increasing drug bio-availability and efficiency while reducing side effects (Molaei, 2019). However, the medicine leaks until it reaches their intended destination as a result of this. The effective target agents such as CQDs are needed as double nano-carrier systems that combine bioimaging and targeted drug delivery vehicle while minimizing cytotoxicity (Qian et al., 2014). CQDs that have been

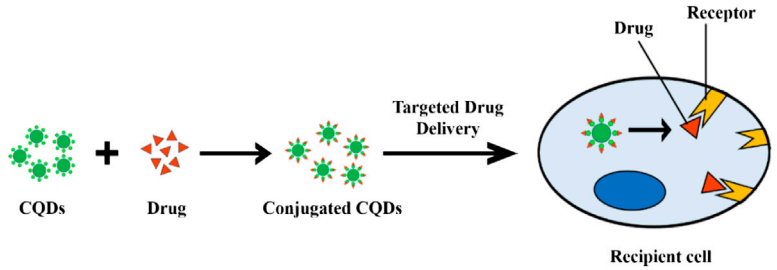

FIGURE 15 | Schematic representation of the CQD-guided drug delivery system.

functionalized can minimize cytotoxicity caused by drug leakage into normal cells.

Amino groups on the surfaces of functionalized CQDs are employed to crosslink with tumor theranostics (Cai et al., 2021). CQDs formed by microwave pyrolysis of citric acid cross-linked with PEGylated oxidized alginate and subsequently conjugated with theranostic doxorubicin (DOX) via acid-labile Schiff base connection. Theranostic nanoparticles were shown *in vitro* to have the ability to release medications in a pH-dependent way in the acidic microenvironment of the tumor (Li G. et al., 2020). Furthermore, their fluorescence enabled imaging-guided drug administration. CQDs have also been utilized to transport drugs to specific parts of the nucleus and mitochondria. Mitochondria are involved in a variety of malignancies and metabolic diseases. When compared to commercially available *MitoTracker* dyes and mitochondrial-specific temperature reliant carrier and receptor-mediated endocytosis, CQDs made from chitosan, ethylenediamine, and mercaptosuccinic acid were found to have lengthy mitochondrial monitoring. CQDs are a good substitute for AuNPs, and varied functionalization could lead to better drug conjugation possibilities in combination with target agents, resulting in a rise in drug delivery decisions, as illustrated in **Figure 15**. The luminescence of CQDs and the site of their emission aid in distinguishing between living and apoptotic cancer cells (Singh et al., 2018). When CQDs included in hydrogel were seen using fluorescence microscopy, they were picked up by A549 cells and emitted green light. The amount of green light emitted related to the concentration level of CQDs in the gel. CQDs obtained from hydrothermal methods were used in a drug delivery mechanism to deliver the anticancer medicine (DOX) to the pointed location. Another study discovered that drug-loaded CQDs were more localized than DOX alone (Li G. et al., 2020). Conjugated CQDs were tested for activity in the body by incubating them in HepG2 and MCF-7 cells. The DOX-conjugated CQDs were found to be more toxic in cancer cells than in normal cells. It is difficult to use in brain tumors and neurological illnesses due to partial brain-impermeability and short medication retention in the brain and blood–brain barrier. As a result, precise tumor cell imaging is necessary for accurate diagnosis and prognosis. CQDs were also utilized to target brain cancers in conjunction with tumor infiltrating peptides (Pardo et al., 2018). To infiltrate the tumor's vascular barriers, RGERPPR-infiltrating peptides (tumor-penetrating peptide) with CQDs were employed. CQDs were hydrothermally synthesized from citric acid and functionalized with maleimide-polyethylene glycol-amino succinimide succinate (Mal-PEG-NHS) and RGERPPR. The nanoparticles that resulted effectively pointed glioma and provided *in-vivo* bioimaging. **Table 3** shows the various drug delivery applications of CQDs with the information of different kinds of drug loaded, and the ligament attached on the CQDs' surface depends upon the targeted cells.

4.6 Solar Cells

Solar cells (SCs) have gone through three generations of growth as of now. The first generation of solar cells is made of crystalline SiO_2 with the core of mono-crystalline SiO_2. However, crystalline SiO_2 is costly, and cell production is expensive. SiO_2, an indirect band-gap material, has a substantially lower absorption coefficient in the visible region than other optoelectronic materials (Green, 2002). Because of these flaws in crystalline SiO_2 SCs, researchers began to look into thin-film SCs, which is entered in the second generation of development. Materials with a high absorption coefficient and a direct band-gap structure are used in thin-film SCs. The benefits of thin-film SCs include their smaller thickness, inexpensive, and various types. There are currently GaAs thin-film SCs, CdTe thin-film SCs, and so on (Imamzai et al., 2012). Thin-film SCs on the other hand have drawbacks such as limited rare-element reserves and arduous mining, and a few are environmentally toxic. Solar cell evolution is now in its third generation with dye-sensitized SCs (DSSCs), polymer SCs, perovskite SCs, and quantum dot SCs. In general, fabrication cost, performance, and durability are used to rank photovoltaic devices. The most significant issue is to balance these factors in photovoltaic devices to have a role in the international energy industry. Despite the many benefits of PSCs, further modifications will be extremely useful for their prospective commercial deployment. Non-toxic materials, reduced charge carrier recombination, manufacturing large-scale production, and improved stability under environmental conditions must also be managed (Shi and Jayatissa, 2018). Perovskite composites are initially employed in the n-i-p FTO/meso-porous scaffold/perovskite materials/hole transport layer (HTL)/metal contact arrangement. However, it requires a high-temperature sintering operation. Furthermore, planar PSCs (in both nip and pin configurations) can be made using a low-temperature technique. As a result of the economic concerns, planar PSCs are preferred. In considerations of both planar as well as

TABLE 3 | Information of various drug delivery applications using CQDs and various synthesis processes.

Carbon materials	Precursor	Synthesis method	Drug loaded	Ligand attached	Targeted cells	Reference
MF-CQDs	Crab shell	One-pot microwave-assisted pyrolysis	Dox	Folic acid@Gd-CODs	HeLa cells	Yao et al. (2017)
TF-CQDs	Citric acid (CA)	Hydrothermal	Dox	Transferrin (TF)	MCF-7 cells	Mahani et al. (2021)
C-dots	CA and o-phenylenediamine	Hydrothermal	Dox	—	HeLa cells	Wang et al. (2016)
C-dots	D-glucose and L-aspartic acid	Straightforward pyrolysis	Dox	Polydopamine (PDA)	HeLa cells	Sun et al. (2017)
C-dots	Carbon nanopowder	—	Dox	Transferrin	CHLA-266, SJGBM2	Li et al. (2016)
C-dots	Sorbitol and sodium hydroxide	Microwave assisted	Dox	Folic acid	HeLa cells	Mewada et al. (2014)
C-dots	Dandelion and the Ethylenediamine (EDA)	Hydrothermal	—	Folic acid	HepG-2	Xuewei Zhao et al. (2017)
C-dots	Hyaluronic acid	Microwave assisted	Gene	Hyaluronan	HeLa cells	Hai-Jiao Wang et al. (2017)
CQDs	CA and EDA	Hydrothermal	—	Quinic acid	Breast cancer cells	Samimi et al. (2021)
Arg-Ag/Cu-CQDs	L-arginine	Hydrothermal	Dox	—	4T1 and HUVEC	Han et al. (2021)
N-CQDs	CA and EDA	Tube furnace thermal synthesis	Dox	D-biotin	HeLa cells	Bao et al. (2019)

Footnotes: MF-CQDs (magneto fluorescent CQDs), TF-CQDs (transferrin-targeted CQDs), and Arg-Ag/Cu-CQDs (CQDs from L-arginine and doped with the duplex metal of Ag/Cu).

mesoscopic structures, the methyl ammonium lead iodide (MAPbI3)-based PSCs are most analyzed light absorbers (Zaman et al., 2017). The creation of a defect at the surface due to iodine and methylamine ion/defect mobility is a significant performance limiting characteristic for organo-halide PSCs. Organic ions escape from perovskite crystalline caused by weak bonding and unstable, which resulted in a non-stoichiometric perovskite layer surface. Due to this process, the non-radiative charge recombination (NCR) occurs at grain-boundaries. NCR reduces the fill factor (FF), lowering the overall energy output that cells can generate. The hysteresis loop of I-V curves is another barrier to commercial viability due to non-uniformity and the surface defects (Girish et al., 2022). Here, the CQDs often have a wide spectrum of light absorption tailing into the visible area, which is advantageous for solar cell applications (SCs). Previously, CQDs were used in a wide range of SCs, along with dye-sensitized SCs, organic SCs, and silicon-based SCs (Meng et al., 2017; You et al., 2020). In a typical perovskite SCs, researchers introduced a sub-monolayer of CQDs between the perovskite and the mesoporous titanium dioxide (TiO_2) layers. In addition, they have used CQDs as an additive for MAPbI3 stabilization via passivation of the perovskite grain boundaries, which improved the power conversion efficiency (PCE) (from 17.59 to 18.81%) and perovskite SC consistency (Guo et al., 2018). The carboxylic, hydroxyl, and amino groups are passivated on the CQDs surface, which made the contacts strong and stable with the uncoordinated Pb in MAPbI3, resulting in a decreased trap-state density and improved optoelectronic characteristics. Furthermore, the interaction between CQDs and MAPbI3 created a protective layer that prevented the perovskite from coming into touch with water, improving SC stability. Kirbiyik et al. reported that hetero-atom doped CQDs (N-CQDs), which was introduced in PSCs to serve as an intermediary, assist in the formation of a dense as well as smooth perovskite layer, which gained PCE of 14% (Kırbıyık et al., 2020). CQDs are considered to be potential replacements to poisonous and fragile inorganic halide perovskite-based solar cells, despite the fact that current research on CQDs in the field of solar cells is scarce, much alone their device efficiency (Paulo et al., 2016). Li et al. reported the electron transport layer (ETL) in planar n-i-p hetero-junction perovskite solar cells (SCs) that play a significant role in energy separation and determines the shape of the perovskite film. CQDs/TiO_2 composite with low visible spectrum absorption was a desirable property for perovskite SCs. We attained an exceptional efficiency of 19% using our innovative CQDs/TiO_2 ETL in combination with a planar n-i-p hetero-junction under stable illumination test circumstances. When compared with TiO_2 alone, a CQDs/TiO_2 combination boosted both the open-circuit voltage and short-circuit current density (Li H. et al., 2017). Zhang et al. reported the N-doped CQDs (NCQDs) that can mix with rutile TiO_2 to create NCQDs/TiO_2 hierarchical nanoparticles built by nanorods with improved photo-catalytic activity, which is demonstrated under visible irradiation. The pseudo first order reaction constants for rhodamine B (RhB) deterioration on NCQDs/TiO_2 ($0.11\ min^{-1}$) are 215.7, 7.3, and 1.3 times greater than those for NCQDs ($0.00051\ min^{-1}$), TiO_2 ($0.015\ min^{-1}$), and CQDs/TiO_2 ($0.086\ min^{-1}$), respectively. The open-circuit voltage and fill factors are 0.46 V and 43% (Zhang et al., 2013). Carolan et al. reported a simply customized atmospheric pressure micro-plasma to make N-CQDs. The band-gap energy structure of N-CQDs is revealed, and they are used as the photo-active layer in a solar cell with an open-circuit voltage of 1.8 V and a PCE of 0.8% (Carolan et al., 2017).

4.6.1 Dye-Sensitized Solar Cells

DSSCs are the third generation of solar cells, and they have sparked a lot of interest because of their versatility, lesser cost, and easy processing (Zhang et al., 2013). Although DSSCs offer more

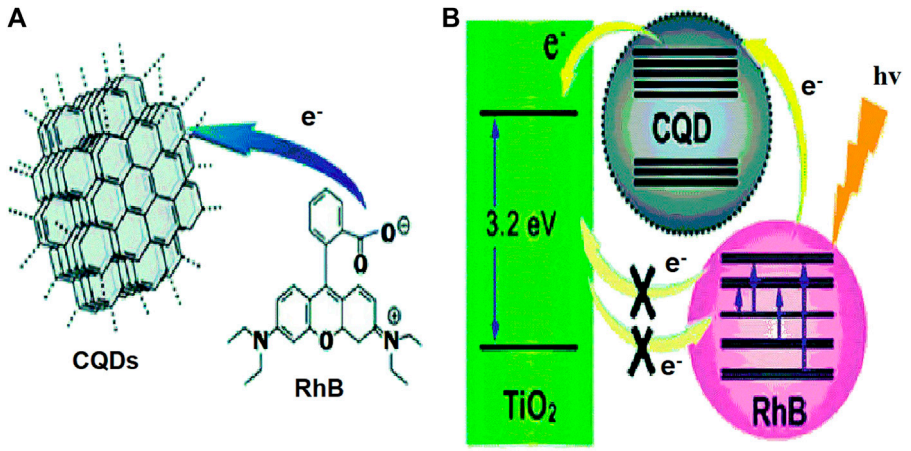

FIGURE 16 | (A) Scheme of electron transfer to CQDs from RhB. **(B)** The CQDs work as an electron transfer mediator. Reprinted with the permission from (Wang and Hu, 2014).

advantages from the multiplicity of organic dyes and achieve desirable performance, photo-bleaching of organic dyes, higher cost, ruthenium-containing dyes (produce toxicity), and volatile electrolyte might have limited their widespread applications. CQDs with consistent optical absorption derived from a wide range of low-cost sources show promise in DSCs (Riaz et al., 2019). A CQD interlinked dye and semiconductor complex system has been established for the development of extremely efficient photoelectric conversion technologies in 2013. Because of the integrated hyper-chromic effect between Rhodamine B (RhB) and CQDs, CQDs not just to increase the UV–visible absorption of RhB solutions (**Figure 16**). The CQDs not only act as an electron transfer mediator (or bridge) between photo-generated electrons and suppress their recombination, but they also efficiently suppressed photo-generated electron recombination, resulting in a greatly improved photoelectric conversion efficiency.

The addition of CQDs to the dye and the semiconductor complex increased the complex's photoelectric conversion efficiency by seven times (Ma et al., 2013).

Geleta et al. reported the nanocomposites of n-type ZnO and p-type NiO semiconductors as photo-anodes in DSSCs to improve PCE. The impact of CQDs on the n-ZnO and p-NiO nanocomposite was also studied. With the incorporation of 8 wt% NiO, the efficiency achieved was 1.58 times than that of ZnO. Furthermore, doping CQDs in ZnO/NiO nanocomposites (8 wt %) increased the efficiency by 3.8 times than ZnO/NiO nanocomposite without doping (Geleta and Imae, 2021). Huang et al. reported for the first time, allium fistulosum as a sensitizer in quantum dot-sensitized solar cells (QDSSCs) to synthesize nitrogen self-doped CQDs using a one-pot hydrothermal technique. CQDs with blue fluorescence have a size of 11.67 nm. The CQDs' HOMO and LUMO levels are −5.22 eV and −3.80 eV, respectively, which corresponded to TiO_2 and the electrolyte energy levels. All of this demonstrated that CQDs might be used as sensitizers in QDSSCs and a 0.45% PCE with a fill factor of 0.60 (Huang et al., 2020b).

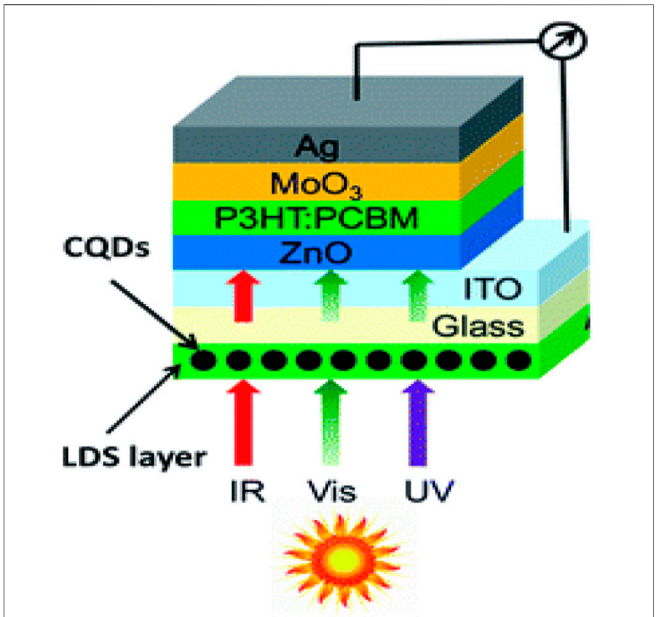

FIGURE 17 | Schematic architecture of the BHJ solar cell with the LDS layer. Reprinted with the permission from (Wang and Hu, 2014).

4.6.2 Organic Solar Cells

Organic solar cells (OSCs) are also called as polymer solar cells. They can be mass-produced on a large scale using the roll-to-roll process and are distinguished by the device's flexibility as well as lower cost (Vercelli, 2021). CQDs have recently been used in organic solar cells as an electron acceptor (eA) (Cui et al., 2018), active-layer dopant (Liu et al., 2014), hole transport layer (HTL) (Li et al., 2013), electron transport layer (ETL) (Pali et al., 2018), and interfacial modification layer (Lin et al., 2016) as well as dopant of buffer layer (Yan et al., 2016), which all illustrated CQDs' excellent applications in OSCs. However, it is important to

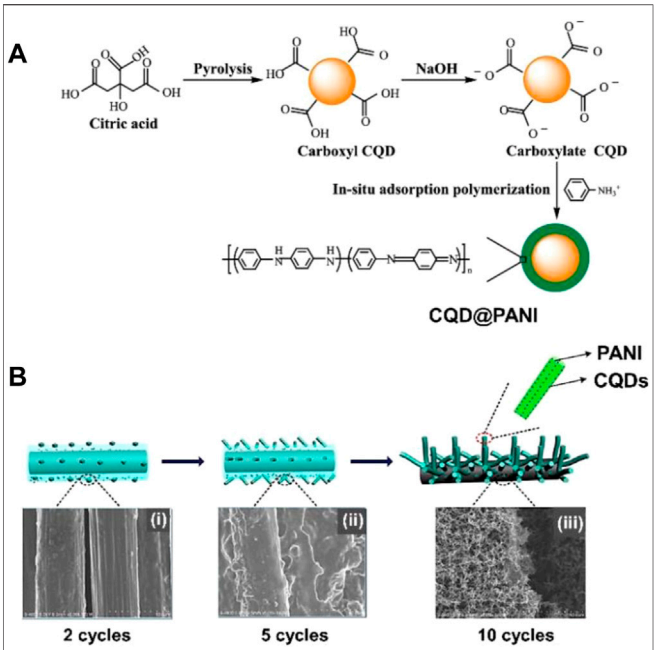

FIGURE 18 | (A) Schematic illustration of the synthesis of core shells C-QDs@PANI by pyrolysis. **(B)** Schematic illustrations and corresponding SEM images of C-QDs@PANI/CFs (LI). Reprinted with the permission from (Permatasari et al., 2021).

note that the majority of CQD synthetic methods for OSCs struggle from stringent operating parameters, which might also restrict their wide practical implementation. However, despite the fact that many researchers have focused on un-doped and N-doped carbon based nanomaterials for its use in OSCs, the studies are reported the hydrothermal synthesis of N,S-CQDs (Riaz and Park, 2022). In OSCs, ZnO is among the most often utilized ETLs. Furthermore, because of several surface imperfections and uneven of energy gaps with the photo-active layer, the ZnO-based cells are normally requiring a light-soaking method to obtain high efficiency of the device.

Wang et al. reported the N,S-CQD-modified ZnO ETL cells that had a higher PCE of 9.31% that was greater than the un-modified ZnO cells (Wang Y. et al., 2019). Zhang et al. reported high performance inverted poly-SCs through the use of a bilayer ZnO/CQDs' electron extraction layer (EEL). The inverted poly-SCs based on a polymer composite blend have a significant enhancement in PCE of 9.64%, which is 27% higher than a control cell of 7.59% (Zhang et al., 2018). On the other hand, the spectral ranges of both PL and excitation of the CQD-filled polysiloxane composite well matched the harvest-spectrum (480–650 nm) and unutilized optical-spectrum (380–480 nm) of the bulk hetero-junction (BHJ) solar cell (Zhang et al., 2017) because the CQD-filled polysiloxane composite may emit light with wavelengths ranging from 400 to 650 nm when excited at 320–450 nm. As the composite's emission wavelength range corresponds to the responding curve of the P3HT:PCBM based BHJ SCs, depositing a layer of the composite on the cover glass can boost power conversion efficiency by roughly 12% as a consequence of enhanced absorbance of near UV and blue/violet part sunlight (**Figure 17**) (Müllerova et al., 2016).

4.7 Supercapacitors

Supercapacitors are unlike batteries, and it is an energy-storage device that hold high output power for extended periods of time (Raza et al., 2018). The development of a nanomaterial-based electrode having a greater specific-capacitance and longer-term consistency is a better alternative for supercapacitors. Despite present efforts, more studies are needed to develop novel porous, conducting, and large surface area carbon products with enhanced specific capacitance as well as cycle stability (Jian et al., 2017; Sahoo et al., 2018). CQDs are often used in supercapacitors because of its size and structure adjustable properties and excellent electrical conductivity. As a result, utilizing metal oxide/sulfide and CQDs to synthesize nanohybrid structures has been demonstrated as a promising technique for creating effective and consistent supercapacitors. An environmentally friendly technique to synthesize CQD-MnO_2 nanostructures from a sustainable waste source to obtain high power density and specific-capacitance was reported. CQD-MnO_2 had a greater surface area and enhanced electrical conductivity compared to virgin MnO_2, as evidenced by the highly conductive CQDs according to the structural investigation (Xu et al., 2017). CQDs can enhance the electrical conductivity of metal oxide/sulfide hybrids while also improving the electrochemical properties of energy storage systems. **Figure 18** shows that the CQDs@PANI composite increases the energy storage density in the supercapacitor. A simple, ecologically friendly, and one-pot synthesis-method has been used to make manganese oxide graphene (MnOx CDGs) nanohybrids. Because of their greater electrical conductivity and higher electrochemical function, transition-metal sulfide is more suitable for use in energy storage technologies from an electronic stand-point.

These characteristics helped to create energy storage systems that are both stable and high-performing. A unique hierarchical porous nano-flower-like nanocomposite in 2020 was reported by incorporation of CQDs into a CuS nanostructure (CuS@CQDs). To make the CuS@CQDs nanocomposite, researchers used two separate methods: the impregnation combined method (ICM) and the solvothermal synthesis method (SSM) (Quan et al., 2020). According to the Brunauer–Emmett–Teller (BET) investigation, these nanocomposites have a surface area of 111.2 m^2g^{-1} when compared to virgin CuS (22.8 m^2g^{-1}). Furthermore, studies of pore-size distributions found that nanocomposites contain a substantial number of mesopore structures. CuS@CQDs nanocomposite electrodes showed a higher specific capacitance and a power density of 920.5 Fg^{-1} and 397.75 Wkg^{-1}, respectively (Rasal et al., 2021). Furthermore, the devices displayed longer period stability with 92.8 percent of its initial effectiveness persisting after 10,000 charge and discharge cycles. According to the structural analyses, these nanocomposites possessed a porous structure with a surface area that was roughly 40% higher than the pure NiS nanostructure. When compared to pure NiS nanostructures, these nanocomposites showed better charge transfer kinetics, surface area, and charge-discharge stability as evidenced by electrochemical experiments (Ouyang et al., 2021). Furthermore, the NiS CQD-based nanocomposite

TABLE 4 | CQD-based nanocomposites and their uses in the fabrication of supercapacitors and comparisons of device performance.

Carbon materials	Precursor	Synthesis method	Specific capacitance ($F\ g^{-1}$)	Energy density (Wh/kg)	Charge-discharge cycles	Reference
MnOx–CDGs	Ammonium citrate	One-pot microwave pyrolysis	~280	—	>10000	Unnikrishnan et al. (2016)
Bi_2O_3–CQD	Spoiled milk	Hydrothermal	~75–300	88	2500	Prasath et al. (2019)
CuS@CQDs	Citric acid and ethylenediamine	One-step solvothermal	920.5	44.19	>10000	Quan et al. (2020)
NiS–CQDs	Lemon juice	Hydrothermal	880	30	2000	Sahoo et al. (2018)
CQDs/ MoS_2@ZnS	Glucose	Hydrothermal	2899.5	33.97	3500	Zheng et al. (2019)
CTSs@CQDs	$SnCl_4{\cdot}5H_2O$, $CuCl_2{\cdot}2H_2O$ and PEG	Hydrothermal	856	—	300	Bi et al. (2019)
rGH/CDs	Glucose	Hydrothermal	264	35.3	5000	Feng et al. (2018)
MoS_2/NCDs	Urea and citric acid	Solvothermal	250.55	20.01	5000	El Sharkawy et al. (2020)
GQD/$CuCo_2S_4$	$Cu(NO_3)_2$,$Co(NO_3)_2$ and GQDs powder	Hydrothermal	1725	—	10,000	Yuanyuan Huang et al. (2019)
PPy/CQDs	Ascorbic acid and polystyrene sulphonic acid	Electro-polymerization	1073.5	—	2000	Malik et al. (2020)

Footnotes: MnOx-CDGs (carbon dots doped manganese Oxide Decorated Graphene Nanosheets), Bi_2O_3-CQDs (bismuth oxide anchored CQDs), CuS@CQDs (copper sulfide nanoflower and CQDs nanocomposite), NiS-CQDs (CQDs incorporated nickel sulfide), CQDs/MoS_2@ZnS (CQD doped molybdenum disulfide and zinc sulfide composite), CTSs@CQDs (copper tin sulfide nanoflower modified CQDs), rGH/CDs (reduced graphene oxide hydrogel CDs), MoS_2/NCDs (molybdenum disulfide and nitrogen doped CDs nanocomposite), GQD/$CuCo_2S_4$ (GQDs doped copper cobalt sulfide), and PPy/CQDs (CQDs intercalated in polypyrrole).

had a greater specific capacitance than pure NiS electrodes. Moreover, the researchers have developed the CQD-based nanohybrids and subjected to characterization technique to measure the specific capacitance, energy storage density, high power density and cycle consistency, as shown in **Table 4**.

5 SUMMARY AND OUTLOOK

The CQDs were invented in 2004 during sanitization of single walled carbon nanotube (SWCNT). From the previous discussion, we noticed that the many researchers have synthesized and developed the CQDs by various methodologies. The CQDs have shown excellent properties such as good biocompatibility, lesser toxic, fluorescent in nature, simple synthesis, good electrical conductivity, and low cost. Therefore, CQDs have been used in many important applications such as sensors, bio-medical, optoelectronics, and energy sectors. However, the result of expectation is not fulfilled and the large-scale production is quite critical. In the future, the CQDs' production must be upgraded by sophisticated synthetic procedures, right elemental doped and right surface passivation. For example, the CQDs were doped to electrically conducting materials to develop the conducting micro-fluid or fluorescent conducting ink for sensor and microelectronic systems (El-Shamy, 2019; Zhou Q. et al., 2021). Because of this type of CQD could be optically fluorescent and electrically conductive, CQD was also used in drug delivery because they have a good biocompatible property. In drug delivery applications, it is used as a carrier because of their fluorescent property. The drug will be delivered to the targeted location as carried by tracking of continuous fluorescence emission. In the case of CQDs doped with electromagnetic or magnetically induced material, then the drug will be delivered to the targeted location with the help of the external magnetic or electromagnetic field by the controlled drug carrier. In supercapacitor application, the CQD was made into a nanohybrid form to make a high-power density and high-energy density supercapacitors. These are all the futuristic development of CQDs.

Recently, CQDs are utilized for energy generation via an osmotic power generation (OPG). In OPG, the pressure retarded osmosis (PRO) is involved to generate the power. The osmotic pressure gradient energy is generated in PRO by combining two different salinities of water. Due to the chemical potential difference across the semipermeable membrane, water quickly permeated from the feed side into pressured salty water in this method. Earlier authors have utilized the thin film composite (TFC) as a main membrane material in the PRO process. They have investigated reverse electro-dialysis (RED) and demonstrated how Gibbs free energy of mixing when fresh river-water flows into sea-water can be used to generate sustainable power (Ingole, 2021). However, with their direct interaction with numerous foulants in raw water, the substrates of PRO membranes are especially prone to fouling. This results in a significant loss of power density and makes commercialization of PRO technology difficult. A simple surface modification method was established to produce a novel type of nanoparticle-modified PRO membranes with antifouling property. Zhao et al. synthesized CQDs with the size of 3.2 nm from citric acid using a thermal pyrolysis method for OPG. They are covalently bonded to the polydopamine (PDA) layer grafted onto the substrate surface of poly (ether sulfone) (PES) membranes. PRO tests at 15 bar further showed that the CQD modified membranes had a significantly greater power density (11.0 vs. 8.8 W/m^2) and water retention after backwash (94 vs. 89%) than the unmodified ones (Zhao D. L. et al., 2017). Gai et al. have used 1.0 M NaCl solution and distilled water as the feed pair for

OPC. They have newly designed TFC membranes with 1 wt% Na^+-modified CQDs that had a peak power density of 34.20 W/m^2 at 23 bar (Gai et al., 2018). To the best of author's knowledge, this was the highest power density reported in the literature for OPG using CQDs. For real time usage, it needed further improvement.

More research is still required on CQDs that have opened up a new option for bio-sensing and organic solar cells for future applications. Even though we are currently capable of understanding CQD synthesis methodologies and their prospective applications in sensors, bio-imaging, drug delivery, solar cells, supercapacitors, DSSCs, etc., more research is still needed. It is difficult to manufacture CQDs in a simple and environmentally friendly method with a predetermined structure and size for advanced research and specific applications. CQDs are expected to have a growing role in analytical and bio-analytical science in the coming years. Nevertheless, CQDs with high QY are uncommon till now. Future studies should be focused on greatly increasing the QY of CQDs, as well as the creation of geometrically, compositionally, and structurally well-defined CQDs. When no size limit is set on CQDs' growth, they expand in incredibly wide ranges. Furthermore, there are unknown features in CQDs that have yet to be studied, which keeps their nanoscale chemical and physical nature unexplained, limiting their use in energy storage devices. Another pressing challenge affecting CQD industrialization and synthesis is that the rapid evolution of their raw material sources. Apart from that, CQDs' ability to cut production costs is limited due to a lack of standardization, which has limited their widespread use and commercialization. To further realize the promise of these increasingly essential carbon materials, we predict the progression of more inexpensive, simple, and novel synthetic technologies, as well as innovative promising uses have to be developed.

AUTHOR CONTRIBUTIONS

VM: conceptualization, methodology, and writing—original draft. DG: visualization, investigation, and reviewing. AS: conceptualization, methodology, supervision, and writing—reviewing and editing.

ACKNOWLEDGMENTS

AS thanks the Science and Engineering Research Board (SERB) for funding through CRG/2021/001517. We thank the Department of Science and Technology (DST) (International Bilateral Cooperation Division), India, for financial support through "INDO-RUSSIA Project (File No. INT/RUS/RFBR/385)."

REFERENCES

Ahirwar, S., Mallick, S., and Bahadur, D. (2017). Electrochemical Method to Prepare Graphene Quantum Dots and Graphene Oxide Quantum Dots. *ACS Omega* 2, 8343–8353. doi:10.1021/acsomega.7b01539

Amjadi, M., Manzoori, J. L., Hallaj, T., and Azizi, N. (2017). Sulfur and Nitrogen Co-doped Carbon Quantum Dots as the Chemiluminescence Probe for Detection of Cu2+ Ions. *J. Luminescence* 182, 246–251. doi:10.1016/j.jlumin.2016.10.021

Arora, N., and Sharma, N. N. (2014). Arc Discharge Synthesis of Carbon Nanotubes: Comprehensive Review. *Diam. Relat. Mater.* 50, 135–150. doi:10.1016/j.diamond.2014.10.001

Arsalani, N., Nezhad-Mokhtari, P., and Jabbari, E. (2019). Microwave-assisted and One-step Synthesis of PEG Passivated Fluorescent Carbon Dots from Gelatin as an Efficient Nanocarrier for Methotrexate Delivery. *Artif. Cells, Nanomedicine, Biotechnol.* 47, 540–547. doi:10.1080/21691401.2018.1562460

Arumugam, N., and Kim, J. (2018). Synthesis of Carbon Quantum Dots from Broccoli and Their Ability to Detect Silver Ions. *Mater. Lett.* 219, 37–40. doi:10.1016/j.matlet.2018.02.043

Arumugham, T., Alagumuthu, M., Amimodu, R. G., Munusamy, S., and Iyer, S. K. (2020). A Sustainable Synthesis of Green Carbon Quantum Dot (CQD) from Catharanthus Roseus (White Flowering Plant) Leaves and Investigation of its Dual Fluorescence Responsive Behavior in Multi-Ion Detection and Biological Applications. *Sustain. Mater. Technol.* 23, e00138. doi:10.1016/j.susmat.2019.e00138

Arunragsa, S., Seekaew, Y., Pon-On, W., and Wongchoosuk, C. (2020). Hydroxyl Edge-Functionalized Graphene Quantum Dots for Gas-Sensing Applications. *Diam. Relat. Mater.* 105, 107790. doi:10.1016/j.diamond.2020.107790

Atchudan, R., Edison, T. N. J. I., Perumal, S., Vinodh, R., Sundramoorthy, A. K., Babu, R. S., et al. (2021a). Leftover Kiwi Fruit Peel-Derived Carbon Dots as a Highly Selective Fluorescent Sensor for Detection of Ferric Ion. *Chemosensors* 9, 166. doi:10.3390/chemosensors9070166

Atchudan, R., Jebakumar Immanuel Edison, T. N., Shanmugam, M., Perumal, S., Somanathan, T., and Lee, Y. R. (2021b). Sustainable Synthesis of Carbon Quantum Dots from Banana Peel Waste Using Hydrothermal Process for *In Vivo* Bioimaging. *Phys. E Low-dimensional Syst. Nanostructures* 126, 114417. doi:10.1016/j.physe.2020.114417

Atchudan, R., Kishore, S. C., Edison, T. N. J. I., Perumal, S., Vinodh, R., Sundramoorthy, A. K., et al. (2021c). Highly Fluorescent Carbon Dots as a Potential Fluorescence Probe for Selective Sensing of Ferric Ions in Aqueous Solution. *Chemosensors* 9, 301. doi:10.3390/chemosensors9110301

Azam, N., Najabat Ali, M., and Javaid Khan, T. (2021). Carbon Quantum Dots for Biomedical Applications: Review and Analysis. *Front. Mat.* 8, 272. doi:10.3389/fmats.2021.700403

Baker, S. N., and Baker, G. A. (2010). Luminescent Carbon Nanodots: Emergent Nanolights. *Angew. Chem. Int. Ed.* 49, 6726–6744. doi:10.1002/anie.200906623

Bao, R., Chen, Z., Zhao, Z., Sun, X., Zhang, J., Hou, L., et al. (2018). Green and Facile Synthesis of Nitrogen and Phosphorus Co-doped Carbon Quantum Dots towards Fluorescent Ink and Sensing Applications. *Nanomaterials* 8, 386. doi:10.3390/nano8060386

Bao, W., Ma, H., Wang, N., and He, Z. (2019). pH-sensitive Carbon Quantum Dots–doxorubicin Nanoparticles for Tumor Cellular Targeted Drug Delivery. *Polym. Adv. Technol.* 30, 2664–2673. doi:10.1002/pat.4696

Başoğlu, A., Ocak, Ü., and Gümrükçüoğlu, A. (2020). Synthesis of Microwave-Assisted Fluorescence Carbon Quantum Dots Using Roasted-Chickpeas and its Applications for Sensitive and Selective Detection of Fe3+ Ions. *J. Fluoresc.* 30, 515–526. doi:10.1007/s10895-019-02428-7

Bi, Z., Huang, L., Shang, C., Wang, X., and Zhou, G. (2019). Stable Copper Tin Sulfide Nanoflower Modified Carbon Quantum Dots for Improved Supercapacitors. *J. Chem.* 2019, 1–5. doi:10.1155/2019/6109758

Cai, R., Xiao, L., Liu, M., Du, F., and Wang, Z. (2021). Recent Advances in Functional Carbon Quantum Dots for Antitumour. *Ijn* Vol. 16, 7195–7229. doi:10.2147/IJN.S334012

Campuzano, S., Yáñez-Sedeño, P., and Pingarrón, J. M. (2019). Carbon Dots and Graphene Quantum Dots in Electrochemical Biosensing. *Nanomaterials* 9, 634. doi:10.3390/nano9040634

Cao, L., Meziani, M. J., Sahu, S., and Sun, Y.-P. (2013). Photoluminescence Properties of Graphene versus Other Carbon Nanomaterials. *Acc. Chem. Res.* 46, 171–180. doi:10.1021/ar300128j

Cao, L., Wang, X., Meziani, M. J., Lu, F., Wang, H., Luo, P. G., et al. (2007). Carbon Dots for Multiphoton Bioimaging. *J. Am. Chem. Soc.* 129, 11318–11319. doi:10.1021/ja073527l

Carbonaro, C., Corpino, R., SalisMocci, F., Mocci, S., Thakkar, C., Olla, P. C., et al. (2019). On the Emission Properties of Carbon Dots: Reviewing Data and Discussing Models. *C* 5, 60. doi:10.3390/c5040060

Carolan, D., Rocks, C., Padmanaban, D. B., Maguire, P., Svrcek, V., and Mariotti, D. (2017). Environmentally Friendly Nitrogen-Doped Carbon Quantum Dots for Next Generation Solar Cells. *Sustain. Energy Fuels* 1, 1611–1619. doi:10.1039/c7se00158d

Chang, Q., 2016, Surface of Solids. 175–225. doi:10.1016/B978-0-12-809315-3.00010-4

Chao-Mujica, F. J., Garcia-Hernández, L., Camacho-López, S., Camacho-López, M., Camacho-López, M. A., Reyes Contreras, D., et al. (2021). Carbon Quantum Dots by Submerged Arc Discharge in Water: Synthesis, Characterization, and Mechanism of Formation. *J. Appl. Phys.* 129, 163301. doi:10.1063/5.0040322

Chauhan, S., Jain, N., and Nagaich, U. (2020). Nanodiamonds with Powerful Ability for Drug Delivery and Biomedical Applications: Recent Updates on *In Vivo* Study and Patents. *J. Pharm. Analysis* 10, 1–12. doi:10.1016/j.jpha.2019.09.003

Chen, H., Gao, Q., Li, J., and Lin, J.-M. (2016). Graphene Materials-Based Chemiluminescence for Sensing. *J. Photochem. Photobiol. C Photochem. Rev.* 27, 54–71. doi:10.1016/j.jphotochemrev.2016.04.003

Chen, Y., Cao, Y., Ma, C., and Zhu, J.-J. (2020). Carbon-based Dots for Electrochemiluminescence Sensing. *Mat. Chem. Front.* 4, 369–385. doi:10.1039/C9QM00572B

Cheng, C., Shi, Y., Li, M., Xing, M., and Wu, Q. (2017). Carbon Quantum Dots from Carbonized Walnut Shells: Structural Evolution, Fluorescence Characteristics, and Intracellular Bioimaging. *Mater. Sci. Eng. C* 79, 473–480. doi:10.1016/j.msec.2017.05.094

Cheng, C., Xing, M., and Wu, Q. (2019). A Universal Facile Synthesis of Nitrogen and Sulfur Co-doped Carbon Dots from Cellulose-Based Biowaste for Fluorescent Detection of Fe3+ Ions and Intracellular Bioimaging. *Mater. Sci. Eng. C* 99, 611–619. doi:10.1016/j.msec.2019.02.003

Chu, K.-W., Lee, S., Chang, C.-J., and Liu, L. (2019). Recent Progress of Carbon Dot Precursors and Photocatalysis Applications. *Polymers* 11, 689. doi:10.3390/polym11040689

Clancy, A. J., Bayazit, M. K., Hodge, S. A., Skipper, N. T., Howard, C. A., and Shaffer, M. S. P. (2018). Charged Carbon Nanomaterials: Redox Chemistries of Fullerenes, Carbon Nanotubes, and Graphenes. *Chem. Rev.* 118, 7363–7408. doi:10.1021/acs.chemrev.8b00128

Cui, B., Yan, L., Gu, H., Yang, Y., Liu, X., Ma, C.-Q., et al. (2018). Fluorescent Carbon Quantum Dots Synthesized by Chemical Vapor Deposition: An Alternative Candidate for Electron Acceptor in Polymer Solar Cells. *Opt. Mater.* 75, 166–173. doi:10.1016/j.optmat.2017.10.010

Cui, L., Ren, X., Wang, J., and Sun, M. (2020). Synthesis of Homogeneous Carbon Quantum Dots by Ultrafast Dual-Beam Pulsed Laser Ablation for Bioimaging. *Mater. Today Nano* 12, 100091. doi:10.1016/j.mtnano.2020.100091

Das, G. S., Shim, J. P., Bhatnagar, A., Tripathi, K. M., and Kim, T. (2019). Biomass-derived Carbon Quantum Dots for Visible-Light-Induced Photocatalysis and Label-free Detection of Fe(III) and Ascorbic Acid. *Sci. Rep.* 9, 15084. doi:10.1038/s41598-019-49266-y

Deng, Y., Chen, M., Chen, G., Zou, W., Zhao, Y., Zhang, H., et al. (2021). Visible-Ultraviolet Upconversion Carbon Quantum Dots for Enhancement of the Photocatalytic Activity of Titanium Dioxide. *ACS Omega* 6, 4247–4254. doi:10.1021/acsomega.0c05182

Desmond, L. J., Phan, A. N., and Gentile, P. (2021). Critical Overview on the Green Synthesis of Carbon Quantum Dots and Their Application for Cancer Therapy. *Environ. Sci. Nano* 8, 848–862. doi:10.1039/d1en00017a

Devi, N. R., Kumar, T. H. V., and Sundramoorthy, A. K. (2018). Electrochemically Exfoliated Carbon Quantum Dots Modified Electrodes for Detection of Dopamine Neurotransmitter. *J. Electrochem. Soc.* 165, G3112–G3119. doi:10.1149/2.0191812jes

Devi, P., Saini, S., and Kim, K.-H. (2019). The Advanced Role of Carbon Quantum Dots in Nanomedical Applications. *Biosens. Bioelectron.* 141, 111158. doi:10.1016/j.bios.2019.02.059

Dey, S., Govindaraj, A., Biswas, K., and Rao, C. N. R. (2014). Luminescence Properties of Boron and Nitrogen Doped Graphene Quantum Dots Prepared from Arc-Discharge-Generated Doped Graphene Samples. *Chem. Phys. Lett.* 595-596 (596), 203–208. doi:10.1016/j.cplett.2014.02.012

Dineshkumar, R., Murugan, N., Abisha Rani, J. M., Arthanareeswari, M., Kamaraj, P., Devikala, S., et al. (2019). Synthesis of Highly Fluorescent Carbon Dots from Plectranthus Amboinicus as a Fluorescent Sensor for Ag+ Ion. *Mat. Res. Express* 6, 104006. doi:10.1088/2053-1591/ab3a7b

Ding, C., Zhu, A., and Tian, Y. (2014). Functional Surface Engineering of C-Dots for Fluorescent Biosensing and *In Vivo* Bioimaging. *Acc. Chem. Res.* 47, 20–30. doi:10.1021/ar400023s

Dong, Y., Chen, C., Lin, J., Zhou, N., Chi, Y., and Chen, G. (2013). Electrochemiluminescence Emission from Carbon Quantum Dot-Sulfite Coreactant System. *Carbon* 56, 12–17. doi:10.1016/j.carbon.2012.12.086

Dong, Y., Wang, R., Li, G., Chen, C., Chi, Y., and Chen, G. (2012). Polyamine-Functionalized Carbon Quantum Dots as Fluorescent Probes for Selective and Sensitive Detection of Copper Ions. *Anal. Chem.* 84, 6220–6224. doi:10.1021/ac3012126

Drummen, G. (2010). Quantum Dots-From Synthesis to Applications in Biomedicine and Life Sciences. *Ijms* 11, 154–163. doi:10.3390/ijms11010154

El Sharkawy, H. M., Dhmees, A. S., Tamman, A. R., El Sabagh, S. M., Aboushahba, R. M., and Allam, N. K. (2020). N-doped Carbon Quantum Dots Boost the Electrochemical Supercapacitive Performance and Cyclic Stability of MoS2. *J. Energy Storage* 27, 101078. doi:10.1016/j.est.2019.101078

El-Shabasy, R. M., Farouk Elsadek, M., Mohamed Ahmed, B., Fawzy Farahat, M., Mosleh, K. N., and Taher, M. M. (2021). Recent Developments in Carbon Quantum Dots: Properties, Fabrication Techniques, and Bio-Applications. *Processes* 9, 388. doi:10.3390/pr9020388

El-Shamy, A. g. (2019). Novel Hybrid Nanocomposite Based on Poly(vinyl Alcohol)/ Carbon Quantum Dots/fullerene (PVA/CQDs/C60) for Thermoelectric Power Applications. *Compos. Part B Eng.* 174, 106993. doi:10.1016/j.compositesb.2019.106993

Farshbaf, M., Davaran, S., Rahimi, F., Annabi, N., Salehi, R., and Akbarzadeh, A. (2017). Carbon Quantum Dots: Recent Progresses on Synthesis, Surface Modification and Applications. *Artif. Cells, Nanomedicine, Biotechnol.* 46, 1331–1348. doi:10.1080/21691401.2017.1377725

Feng, H., Xie, P., Xue, S., Li, L., Hou, X., Liu, Z., et al. (2018). Synthesis of Three-Dimensional Porous Reduced Graphene Oxide Hydrogel/carbon Dots for High-Performance Supercapacitor. *J. Electroanal. Chem.* 808, 321–328. doi:10.1016/j.jelechem.2017.12.046

Feng, X., and Zhang, Y. (2019). A Simple and Green Synthesis of Carbon Quantum Dots from Coke for White Light-Emitting Devices. *RSC Adv.* 9, 33789–33793. doi:10.1039/c9ra06946a

Gai, W., Zhao, D. L., and Chung, T.-S. (2018). Novel Thin Film Composite Hollow Fiber Membranes Incorporated with Carbon Quantum Dots for Osmotic Power Generation. *J. Membr. Sci.* 551, 94–102. doi:10.1016/j.memsci.2018.01.034

Galstyan, V. (2017). Porous TiO2-Based Gas Sensors for Cyber Chemical Systems to Provide Security and Medical Diagnosis. *Sensors* 17, 2947. doi:10.3390/s17122947

Geleta, T. A., and Imae, T. (2021). Nanocomposite Photoanodes Consisting of P-NiO/n-ZnO Heterojunction and Carbon Quantum Dot Additive for Dye-Sensitized Solar Cells. *ACS Appl. Nano Mat.* 4, 236–249. doi:10.1021/acsanm.0c02547

Georgakilas, V., Perman, J. A., Tucek, J., and Zboril, R. (2015). Broad Family of Carbon Nanoallotropes: Classification, Chemistry, and Applications of Fullerenes, Carbon Dots, Nanotubes, Graphene, Nanodiamonds, and Combined Superstructures. *Chem. Rev.* 115, 4744–4822. doi:10.1021/cr500304f

Girish, K. H., Vishnumurthy, K. A., and Roopa, T. S. (2022). Role of Conducting Polymers in Enhancing the Stability and Performance of Perovskite Solar Cells: a Brief Review. *Mater. Today Sustain.* 17, 100090. doi:10.1016/j.mtsust.2021.100090

Green, M. A. (2002). Third Generation Photovoltaics: Solar Cells for 2020 and beyond. *Phys. E Low-dimensional Syst. Nanostructures* 14, 65–70. doi:10.1016/S1386-9477(02)00361-2

Guo, Q., Yuan, F., Zhang, B., Zhou, S., Zhang, J., Bai, Y., et al. (2018). Passivation of the Grain Boundaries of CH3NH3PbI3 Using Carbon Quantum Dots for Highly Efficient Perovskite Solar Cells with Excellent Environmental Stability. *Nanoscale* 11, 115–124. doi:10.1039/C8NR08295B

Hallaj, T., Amjadi, M., Manzoori, J. L., and Azizi, N. (2017). A Novel Chemiluminescence Sensor for the Determination of Indomethacin Based on Sulfur and Nitrogen Co-doped Carbon Quantum Dot-KMnO 4 Reaction. *Luminescence* 32, 1174–1179. doi:10.1002/bio.3306

Han, C., Zhang, X., Wang, F., Yu, Q., Chen, F., Shen, D., et al. (2021). Duplex Metal Co-doped Carbon Quantum Dots-Based Drug Delivery System with Intelligent Adjustable Size as Adjuvant for Synergistic Cancer Therapy. *Carbon* 183, 789–808. doi:10.1016/j.carbon.2021.07.063

Han, T., Yan, T., Li, Y., Cao, W., Pang, X., Huang, Q., et al. (2015). Eco-friendly Synthesis of Electrochemiluminescent Nitrogen-Doped Carbon Quantum Dots from Diethylene Triamine Pentacetate and Their Application for Protein Detection. *Carbon* 91, 144–152. doi:10.1016/j.carbon.2015.04.053

Hassan, A. I., and Saleh, H. M. (2021). Quantum Dots: Properties and Applications. *Quantum Dots Prop. Appl.* 96, 331–348. doi:10.21741/9781644901250-13

He, M., Zhang, J., Wang, H., Kong, Y., Xiao, Y., and Xu, W. (2018). Material and Optical Properties of Fluorescent Carbon Quantum Dots Fabricated from Lemon Juice via Hydrothermal Reaction. *Nanoscale Res. Lett.* 13, 175. doi:10.1186/s11671-018-2581-7

Hola, K., Bourlinos, A. B., Kozak, O., Berka, K., Siskova, K. M., Havrdova, M., et al. (2014). Photoluminescence Effects of Graphitic Core Size and Surface Functional Groups in Carbon Dots: COO− Induced Red-Shift Emission. *Carbon* 70, 279–286. doi:10.1016/j.carbon.2014.01.008

Holá, K., Sudolská, M., Kalytchuk, S., Nachtigallová, D., Rogach, A. L., Otyepka, M., et al. (2017). Graphitic Nitrogen Triggers Red Fluorescence in Carbon Dots. *ACS Nano* 11, 12402–12410. doi:10.1021/acsnano.7b06399

Hong, G., Diao, S., Antaris, A. L., and Dai, H. (2015). Carbon Nanomaterials for Biological Imaging and Nanomedicinal Therapy. *Chem. Rev.* 115, 10816–10906. doi:10.1021/acs.chemrev.5b00008

Hou, Y., Lu, Q., Deng, J., Li, H., and Zhang, Y. (2015). One-pot Electrochemical Synthesis of Functionalized Fluorescent Carbon Dots and Their Selective Sensing for Mercury Ion. *Anal. Chim. Acta* 866, 69–74. doi:10.1016/j.aca.2015.01.039

Hu, S.-L., Niu, K.-Y., Sun, J., Yang, J., Zhao, N.-Q., and Du, X.-W. (2009). One-step Synthesis of Fluorescent Carbon Nanoparticles by Laser Irradiation. *J. Mat. Chem.* 19, 484–488. doi:10.1039/B812943F

Hu, S., Liu, J., Yang, J., Wang, Y., and Cao, S. (2011). Laser Synthesis and Size Tailor of Carbon Quantum Dots. *J. Nanopart Res.* 13, 7247–7252. doi:10.1007/s11051-011-0638-y

Huang, C., Dong, H., Su, Y., Wu, Y., Narron, R., and Yong, Q. (2019). Synthesis of Carbon Quantum Dot Nanoparticles Derived from Byproducts in Bio-Refinery Process for Cell Imaging and *In Vivo* Bioimaging. *Nanomaterials* 9, 387. doi:10.3390/nano9030387

Huang, P., Xu, S., Zhang, M., Zhong, W., Xiao, Z., and Luo, Y. (2020a). Carbon Quantum Dots Improving Photovoltaic Performance of CdS Quantum Dot-Sensitized Solar Cells. *Opt. Mater.* 110, 110535. doi:10.1016/j.optmat.2020.110535

Huang, P., Xu, S., Zhang, M., Zhong, W., Xiao, Z., and Luo, Y. (2020b). Green Allium Fistulosum Derived Nitrogen Self-Doped Carbon Dots for Quantum Dot-Sensitized Solar Cells. *Mater. Chem. Phys.* 240, 122158. doi:10.1016/j.matchemphys.2019.122158

Huang, Y., Lin, L., Shi, T., Cheng, S., Zhong, Y., Chen, C., et al. (2019). Graphene Quantum Dots-Induced Morphological Changes in CuCo2S4 Nanocomposites for Supercapacitor Electrodes with Enhanced Performance. *Appl. Surf. Sci.* 463, 498–503. doi:10.1016/j.apsusc.2018.08.247

Huo, X., Liu, L., Bai, Y., Qin, J., Yuan, L., and Feng, F. (2022). Facile Synthesis of Yellowish-Green Emitting Carbon Quantum Dots and Their Applications for Phoxim Sensing and Cellular Imaging. *Anal. Chim. Acta* 1206, 338685. doi:10.1016/j.aca.2021.338685

Iannazzo, D., Pistone, A., Ferro, S., De Luca, L., Monforte, A. M., Romeo, R., et al. (2018). Graphene Quantum Dots Based Systems as HIV Inhibitors. *Bioconjugate Chem.* 29, 3084–3093. doi:10.1021/acs.bioconjchem.8b00448

Imamzai, M., Aghaei, M., Thayoob, Y. H. M., and Forouzanfar, M. (2012). "A Review on Comparison between Traditional Silicon Solar Cells and Thin-Film CdTe Solar Cells," in *Proceedings of National Graduate Conference (Nat-Grad)*. Putrajaya, Malaysia: Tenaga Nasional Universiti, 1–5.

Ingole, P. G. (2020). "Generation of Osmotic Power from Membrane Technology," in *Alternative Energy Resources. The Handbook of Environmental Chemistry*. Editors P. Pathak and R. R. Srivastava (Cham: Springer), Vol.99, 253–271. doi:10.1007/698_2020_632

Jamaludin, N., Rashid, S. A., and Tan, T. (2019). "Natural Biomass as Carbon Sources for the Synthesis of Photoluminescent Carbon Dots," in *Micro and Nano Technologies, Synthesis, Technology and Applications of Carbon Nanomaterials*. Editors S. Abdul Rashid, R. N. I. R. Othman, and M. Z. Hussein (Amsterdam: Elsevier), 109–134. doi:10.1016/B978-0-12-815757-2.00005-X

Jeevanandam, J., Barhoum, A., Chan, Y. S., Dufresne, A., and Danquah, M. K. (2018). Review on Nanoparticles and Nanostructured Materials: History, Sources, Toxicity and Regulations. *Beilstein J. Nanotechnol.* 9, 1050–1074. doi:10.3762/bjnano.9.98

Jia, X., Li, J., and Wang, E. (2012). One-pot Green Synthesis of Optically pH-Sensitive Carbon Dots with Upconversion Luminescence. *Nanoscale* 4, 5572–5575. doi:10.1039/C2NR31319G

Jian, X., Yang, H.-m., Li, J.-g., Zhang, E.-h., Cao, L.-l., and Liang, Z.-h. (2017). Flexible All-Solid-State High-Performance Supercapacitor Based on Electrochemically Synthesized Carbon Quantum Dots/polypyrrole Composite Electrode. *Electrochimica Acta* 228, 483–493. doi:10.1016/j.electacta.2017.01.082

Jiang, Y., Han, Q., Jin, C., Zhang, J., and Wang, B. (2015). A Fluorescence Turn-Off Chemosensor Based on N-Doped Carbon Quantum Dots for Detection of Fe3+ in Aqueous Solution. *Mater. Lett.* 141, 366–368. doi:10.1016/j.matlet.2014.10.168

Kang, C., Huang, Y., Yang, H., Yan, X. F., and Chen, Z. P. (2020). A Review of Carbon Dots Produced from Biomass Wastes. *Nanomaterials* 10, 2316–2324. doi:10.3390/nano10112316

Khan, W. U., Wang, D., Zhang, W., Tang, Z., Ma, X., Ding, X., et al. (2017). High Quantum Yield Green-Emitting Carbon Dots for Fe(III) Detection, Biocompatible Fluorescent Ink and Cellular Imaging. *Sci. Rep.* 7, 14866. doi:10.1038/s41598-017-15054-9

Kırbıyık, Ç., Toprak, A., Başlak, C., Kuş, M., and Ersöz, M. (2020). Nitrogen-doped CQDs to Enhance the Power Conversion Efficiency of Perovskite Solar Cells via Surface Passivation. *J. Alloys Compd.* 832, 154897. doi:10.1016/j.jallcom.2020.154897

Kumari, A., Kumar, A., Sahu, S. K., and Kumar, S. (2018). Synthesis of Green Fluorescent Carbon Quantum Dots Using Waste Polyolefins Residue for Cu2+ Ion Sensing and Live Cell Imaging. *Sensors Actuators B Chem.* 254, 197–205. doi:10.1016/j.snb.2017.07.075

Li, D., Sun, Y., Shen, Q., Zhang, Q., Huang, W., Kang, Q., et al. (2020). Smartphone-based Three-Channel Ratiometric Fluorescent Device and Application in Filed Analysis of Hg2+, Fe3+ and Cu2+ in Water Samples. *Microchem. J.* 152, 104423. doi:10.1016/j.microc.2019.104423

Li, G., Pei, M., and Liu, P. (2020). DOX-conjugated CQD-Based Nanosponges for Tumor Intracellular pH-Triggered DOX Release and Imaging. *Colloids Surfaces A Physicochem. Eng. Aspects* 603, 125258. doi:10.1016/j.colsurfa.2020.125258

Li, H., Shi, W., Huang, W., Yao, E. P., Han, J., Chen, Z., et al. (2017). Carbon Quantum Dots/TiOx Electron Transport Layer Boosts Efficiency of Planar Heterojunction Perovskite Solar Cells to 19. *Nano Lett.* 17, 2328–2335. doi:10.1021/acs.nanolett.6b05177

Li, H., He, X., Kang, Z., Huang, H., Liu, Y., Liu, J., et al. (2010). Water-Soluble Fluorescent Carbon Quantum Dots and Photocatalyst Design. *Angew. Chem. Int. Ed.* 49, 4430–4434. doi:10.1002/anie.200906154

Li, H., Kang, Z., Liu, Y., and Lee, S.-T. (2012). Carbon Nanodots: Synthesis, Properties and Applications. *J. Mat. Chem.* 22, 24230–24253. doi:10.1039/C2JM34690G

Li, L., Yu, B., and You, T. (2015). Nitrogen and Sulfur Co-doped Carbon Dots for Highly Selective and Sensitive Detection of Hg (II) Ions. *Biosens. Bioelectron.* 74, 263–269. doi:10.1016/j.bios.2015.06.050

Li, M., Ni, W., Kan, B., Wan, X., Zhang, L., Zhang, Q., et al. (2013). Graphene Quantum Dots as the Hole Transport Layer Material for High-Performance

Organic Solar Cells. *Phys. Chem. Chem. Phys.* 15, 18973–18978. doi:10.1039/c3cp53283f

Li, S., Amat, D., Peng, Z., Vanni, S., Raskin, S., De Angulo, G., et al. (2016). Transferrin Conjugated Nontoxic Carbon Dots for Doxorubicin Delivery to Target Pediatric Brain Tumor Cells. *Nanoscale* 8, 16662–16669. doi:10.1039/C6NR05055G

Li, S., Zhou, S., Li, Y., Li, X., Zhu, J., Fan, L., et al. (2017). Exceptionally High Payload of the IR780 Iodide on Folic Acid-Functionalized Graphene Quantum Dots for Targeted Photothermal Therapy. *ACS Appl. Mat. Interfaces* 9, 22332–22341. doi:10.1021/acsami.7b07267

Li, X., Rui, M., Song, J., Shen, Z., and Zeng, H. (2015). Carbon and Graphene Quantum Dots for Optoelectronic and Energy Devices: A Review. *Adv. Funct. Mat.* 25, 4929–4947. doi:10.1002/adfm.201501250

Li, X., Wang, H., Shimizu, Y., Pyatenko, A., Kawaguchi, K., and Koshizaki, N. (2011). Preparation of Carbon Quantum Dots with Tunable Photoluminescence by Rapid Laser Passivation in Ordinary Organic Solvents. *Chem. Commun.* 47, 932–934. doi:10.1039/C0CC03552A

Lim, S. Y., Shen, W., and Gao, Z. (2015). Carbon Quantum Dots and Their Applications. *Chem. Soc. Rev.* 44, 362–381. doi:10.1039/c4cs00269e

Lin, H.-S., Jeon, I., Xiang, R., Seo, S., Lee, J.-W., Li, C., et al. (2018). Achieving High Efficiency in Solution-Processed Perovskite Solar Cells Using C60/C70 Mixed Fullerenes. *ACS Appl. Mat. Interfaces* 10, 39590–39598. doi:10.1021/acsami.8b11049

Lin, X., Yang, Y., Nian, L., Su, H., Ou, J., Yuan, Z., et al. (2016). Interfacial Modification Layers Based on Carbon Dots for Efficient Inverted Polymer Solar Cells Exceeding 10% Power Conversion Efficiency. *Nano Energy* 26, 216–223. doi:10.1016/j.nanoen.2016.05.011

Lin, Z., Xue, W., Chen, H., and Lin, J.-M. (2012). Classical Oxidant Induced Chemiluminescence of Fluorescent Carbon Dots. *Chem. Commun.* 48, 1051–1053. doi:10.1039/C1CC15290D

Liu, C., Chang, K., Guo, W., Li, H., Shen, L., Chen, W., et al. (2014). Improving Charge Transport Property and Energy Transfer with Carbon Quantum Dots in Inverted Polymer Solar Cells. *Appl. Phys. Lett.* 105, 073306. doi:10.1063/1.4893994

Liu, H., Xu, H., and Li, H. (2022). Detection of Fe3+ and Hg2+ Ions by Using High Fluorescent Carbon Dots Doped with S and N as Fluorescence Probes. *J. Fluoresc.* 32, 1089–1098. doi:10.1007/s10895-022-02921-6

Liu, J., Li, R., and Yang, B. (2020). Carbon Dots: A New Type of Carbon-Based Nanomaterial with Wide Applications. *ACS Cent. Sci.* 6, 2179–2195. doi:10.1021/acscentsci.0c01306

Liu, M., Xu, Y., Niu, F., Gooding, J. J., and Liu, J. (2016). Carbon Quantum Dots Directly Generated from Electrochemical Oxidation of Graphite Electrodes in Alkaline Alcohols and the Applications for Specific Ferric Ion Detection and Cell Imaging. *Analyst* 141, 2657–2664. doi:10.1039/C5AN02231B

Liu, Y., Li, W., Wu, P., Ma, C., Wu, X., Xu, M., et al. (2019). Hydrothermal Synthesis of Nitrogen and Boron Co-doped Carbon Quantum Dots for Application in Acetone and Dopamine Sensors and Multicolor Cellular Imaging. *Sensors Actuators B Chem.* 281, 34–43. doi:10.1016/j.snb.2018.10.075

Lu, S., Sui, L., Wu, M., Zhu, S., Yong, X., and Yang, B. (2019). Graphitic Nitrogen and High-Crystalline Triggered Strong Photoluminescence and Room-Temperature Ferromagnetism in Carbonized Polymer Dots. *Adv. Sci.* 6, 1801192. doi:10.1002/advs.201801192

Lu, Z., Raad, R., Safaei, F., Xi, J., Liu, Z., and Foroughi, J. (2019). Carbon Nanotube Based Fiber Supercapacitor as Wearable Energy Storage. *Front. Mat.* 6, 138. doi:10.3389/fmats.2019.00138

Ma, Z., Zhang, Y.-L., Wang, L., Ming, H., Li, H., Zhang, X., et al. (2013). Bioinspired Photoelectric Conversion System Based on Carbon-Quantum-Dot-Doped Dye-Semiconductor Complex. *ACS Appl. Mat. Interfaces* 5, 5080–5084. doi:10.1021/am400930h

Mahani, M., Pourrahmani-Sarbanani, M., Yoosefian, M., Divsar, F., Mousavi, S. M., and Nomani, A. (2021). Doxorubicin Delivery to Breast Cancer Cells with Transferrin-Targeted Carbon Quantum Dots: An *In Vitro* and In Silico Study. *J. Drug Deliv. Sci. Technol.* 62, 102342. doi:10.1016/j.jddst.2021.102342

Maiti, D., Tong, X., Mou, X., and Yang, K. (2019). Carbon-Based Nanomaterials for Biomedical Applications: A Recent Study. *Front. Pharmacol.* 9, 1401. doi:10.3389/fphar.2018.01401

Malik, R., Lata, S., Soni, U., Rani, P., and Malik, R. S. (2020). Carbon Quantum Dots Intercalated in Polypyrrole (PPy) Thin Electrodes for Accelerated Energy Storage. *Electrochimica Acta* 364, 137281. doi:10.1016/j.electacta.2020.137281

Marković, Z. M., Labudová, M., Danko, M., Matijašević, D., Mičušík, M., Nádaždy, V., et al. (2020). Highly Efficient Antioxidant F- and Cl-Doped Carbon Quantum Dots for Bioimaging. *ACS Sustain. Chem. Eng.* 8, 16327–16338. doi:10.1021/acssuschemeng.0c06260

Martynenko, I. V., Litvin, A. P., Purcell-Milton, F., Baranov, A. V., Fedorov, A. V., and Gun'ko, Y. K. (2017). Application of Semiconductor Quantum Dots in Bioimaging and Biosensing. *J. Mat. Chem. B* 5, 6701–6727. doi:10.1039/C7TB01425B

Matea, C., Mocan, T., Tabaran, F., Pop, T., Mosteanu, O., Puia, C., et al. (2017). Quantum Dots in Imaging, Drug Delivery and Sensor Applications. *Ijn* Vol. 12, 5421–5431. doi:10.2147/IJN.S138624

Meng, Y., Zhang, Y., Sun, W., Wang, M., He, B., Chen, H., et al. (2017). Biomass Converted Carbon Quantum Dots for All-Weather Solar Cells. *Electrochimica Acta* 257, 259–266. doi:10.1016/j.electacta.2017.10.086

Mewada, A., Pandey, S., Thakur, M., Jadhav, D., and Sharon, M. (2014). Swarming Carbon Dots for Folic Acid Mediated Delivery of Doxorubicin and Biological Imaging. *J. Mat. Chem. B* 2, 698–705. doi:10.1039/C3TB21436B

Miao, X., Qu, D., Yang, D., Nie, B., Zhao, Y., Fan, H., et al. (2018). Synthesis of Carbon Dots with Multiple Color Emission by Controlled Graphitization and Surface Functionalization. *Adv. Mat.* 30, 1704740. doi:10.1002/adma.201704740

Molaei, M. J. (2019). Carbon Quantum Dots and Their Biomedical and Therapeutic Applications: A Review. *RSC Adv.* 9, 6460–6481. doi:10.1039/c8ra08088g

Molaei, M. J. (2020). Principles, Mechanisms, and Application of Carbon Quantum Dots in Sensors: a Review. *Anal. Methods* 12, 1266–1287. doi:10.1039/C9AY02696G

Monte-Filho, S. S., Andrade, S. I. E., Lima, M. B., and Araujo, M. C. U. (2019). Synthesis of Highly Fluorescent Carbon Dots from Lemon and Onion Juices for Determination of Riboflavin in Multivitamin/mineral Supplements. *J. Pharm. Analysis* 9, 209–216. doi:10.1016/j.jpha.2019.02.003

Müllerová, J., Kaiser, M., Nádaždy, V., Šiffalovič, P., and Majková, E. (2016). Optical Absorption Study of P3HT:PCBM Blend Photo-Oxidation for Bulk Heterojunction Solar Cells. *Sol. Energy* 134, 294–301. doi:10.1016/j.solener.2016.05.009

Murugan, N., Prakash, M., Jayakumar, M., Sundaramurthy, A., and Sundramoorthy, A. K. (2019). Green Synthesis of Fluorescent Carbon Quantum Dots from Eleusine Coracana and Their Application as a Fluorescence 'turn-Off' Sensor Probe for Selective Detection of Cu2+. *Appl. Surf. Sci.* 476, 468–480. doi:10.1016/j.apsusc.2019.01.090

Murugan, N., and Sundramoorthy, A. K. (2018). Green Synthesis of Fluorescent Carbon Dots from Borassus Flabellifer Flowers for Label-free Highly Selective and Sensitive Detection of Fe3+ Ions. *New J. Chem.* 42, 13297–13307. doi:10.1039/C8NJ01894D

Nakano, K., Honda, T., Yamasaki, K., Tanaka, Y., Taniguchi, K., Ishimatsu, R., et al. (2018). Carbon Quantum Dots as Fluorescent Component in Peroxyoxalate Chemiluminescence for Hydrogen Peroxide Determination. *Bcsj* 91, 1128–1130. doi:10.1246/bcsj.20180095

Namdari, P., Negahdari, B., and Eatemadi, A. (2017). Synthesis, Properties and Biomedical Applications of Carbon-Based Quantum Dots: An Updated Review. *Biomed. Pharmacother.* 87, 209–222. doi:10.1016/j.biopha.2016.12.108

Nasrin, A., Hassan, M., Mann, G., and Gomes, V. G. (2020). Conjugated Ternary Doped Carbon Dots from Vitamin B Derivative: Multispectral Nanoprobes for Targeted Melanoma Bioimaging and Photosensitization. *J. Luminescence* 217, 116811. doi:10.1016/j.jlumin.2019.116811

Nikolic, M. V., Milovanovic, V., Vasiljevic, Z. Z., and Stamenkovic, Z. (2020). Semiconductor Gas Sensors: Materials, Technology, Design, and Application. *Sensors* 20, 6694. doi:10.3390/s20226694

Niu, F., Xu, Y., Liu, J., Song, Z., Liu, M., and Liu, J. (2017). Controllable Electrochemical/electroanalytical Approach to Generate Nitrogen-Doped Carbon Quantum Dots from Varied Amino Acids: Pinpointing the Utmost Quantum Yield and the Versatile Photoluminescent and Electrochemiluminescent Applications. *Electrochimica Acta* 236, 239–251. doi:10.1016/j.electacta.2017.03.085

Oh, E., Hong, M.-Y., Lee, D., Nam, S.-H., Yoon, H. C., and Kim, H.-S. (2005). Inhibition Assay of Biomolecules Based on Fluorescence Resonance Energy Transfer (FRET) between Quantum Dots and Gold Nanoparticles. *J. Am. Chem. Soc.* 127, 3270–3271. doi:10.1021/ja0433323

Ouyang, Y., Chen, Y., Peng, J., Yang, J., Wu, C., Chang, B., et al. (2021). Nickel Sulfide/activated Carbon Nanotubes Nanocomposites as Advanced Electrode of High-Performance Aqueous Asymmetric Supercapacitors. *J. Alloys Compd.* 885, 160979. doi:10.1016/j.jallcom.2021.160979

Pali, L. S., Gupta, S. K., and Garg, A. (2018). Organic Solar Cells on Al Electroded Opaque Substrates: Assessing the Need of ZnO as Electron Transport Layer. *Sol. Energy* 160, 396–403. doi:10.1016/j.solener.2017.12.028

Pardo, J., Peng, Z., and Leblanc, R. (2018). Cancer Targeting and Drug Delivery Using Carbon-Based Quantum Dots and Nanotubes. *Molecules* 23, 378. doi:10.3390/molecules23020378

Paulo, S., Stoica, G., Cambarau, W., Martinez-Ferrero, E., and Palomares, E. (2016). Carbon Quantum Dots as New Hole Transport Material for Perovskite Solar Cells. *Synth. Met.* 222, 17–22. doi:10.1016/j.synthmet.2016.04.025

Permatasari, F. A., Irham, M. A., Bisri, S. Z., and Iskandar, F. (2021). Carbon-Based Quantum Dots for Supercapacitors: Recent Advances and Future Challenges. *Nanomaterials* 11, 91. doi:10.3390/nano11010091

Pillar-Little, T. J., Wanninayake, N., Nease, L., Heidary, D. K., Glazer, E. C., and Kim, D. Y. (2018). Superior Photodynamic Effect of Carbon Quantum Dots through Both Type I and Type II Pathways: Detailed Comparison Study of Top-Down-Synthesized and Bottom-Up-Synthesized Carbon Quantum Dots. *Carbon* 140, 616–623. doi:10.1016/j.carbon.2018.09.004

Prajapati, H. N., Khiriya, P. K., Tripathi, G. K., Bundela, P., and Khare, P. S. (2021). Green Synthesis of SnO2/Carbon Quantum Dots Nanocomposite for Gas Sensing Application. *Int. J. Res. Rev.* 8, 332–336. doi:10.52403/ijrr.20210746

Prasannan, A., and Imae, T. (2013). One-Pot Synthesis of Fluorescent Carbon Dots from Orange Waste Peels. *Ind. Eng. Chem. Res.* 52, 15673–15678. doi:10.1021/ie402421s

Prasath, A., Athika, M., Duraisamy, E., Selva Sharma, A., Sankar Devi, V., and Elumalai, P. (2019). Carbon Quantum Dot-Anchored Bismuth Oxide Composites as Potential Electrode for Lithium-Ion Battery and Supercapacitor Applications. *ACS Omega* 4, 4943–4954. doi:10.1021/acsomega.8b03490

Pu, Z.-F., Wen, Q.-L., Yang, Y.-J., Cui, X.-M., Ling, J., Liu, P., et al. (2020). Fluorescent Carbon Quantum Dots Synthesized Using Phenylalanine and Citric Acid for Selective Detection of Fe3+ Ions. *Spectrochimica Acta Part A Mol. Biomol. Spectrosc.* 229, 117944. doi:10.1016/j.saa.2019.117944

Qian, Z., Shan, X., Chai, L., Ma, J., Chen, J., and Feng, H. (2014). Si-Doped Carbon Quantum Dots: A Facile and General Preparation Strategy, Bioimaging Application, and Multifunctional Sensor. *ACS Appl. Mat. Interfaces* 6, 6797–6805. doi:10.1021/am500403n

Qin, D., Jiang, X., Mo, G., Feng, J., Yu, C., and Deng, B. (2019). A Novel Carbon Quantum Dots Signal Amplification Strategy Coupled with Sandwich Electrochemiluminescence Immunosensor for the Detection of CA15-3 in Human Serum. *ACS Sens.* 4, 504–512. doi:10.1021/acssensors.8b01607

Quan, Y., Wang, G., Lu, L., Wang, Z., Xu, H., Liu, S., et al. (2020). High-performance Pseudo-capacitor Energy Storage Device Based on a Hollow-Structured Copper Sulfide Nanoflower and Carbon Quantum Dot Nanocomposite. *Electrochimica Acta* 353, 136606. doi:10.1016/j.electacta.2020.136606

Rao, R., Pint, C. L., Islam, A. E., Weatherup, R. S., Hofmann, S., Meshot, E. R., et al. (2018). Carbon Nanotubes and Related Nanomaterials: Critical Advances and Challenges for Synthesis toward Mainstream Commercial Applications. *ACS Nano* 12, 11756–11784. doi:10.1021/acsnano.8b06511

Rasal, A. S., Yadav, S., Yadav, A., Kashale, A. A., Manjunatha, S. T., Altaee, A., et al. (2021). Carbon Quantum Dots for Energy Applications: A Review. *ACS Appl. Nano Mat.* 4, 6515–6541. doi:10.1021/acsanm.1c01372

Raza, W., Ali, F., Raza, N., Luo, Y., Kim, K.-H., Yang, J., et al. (2018). Recent Advancements in Supercapacitor Technology. *Nano Energy* 52, 441–473. doi:10.1016/j.nanoen.2018.08.013

Ren, X., Zhang, F., Guo, B., Gao, N., and Zhang, X. (2019). Synthesis of N-Doped Micropore Carbon Quantum Dots with High Quantum Yield and Dual-Wavelength Photoluminescence Emission from Biomass for Cellular Imaging. *Nanomaterials* 9, 495. doi:10.3390/nano9040495

Riaz, R., Ali, M., Maiyalagan, T., Anjum, A. S., Lee, S., Ko, M. J., et al. (2019). Dye-sensitized Solar Cell (DSSC) Coated with Energy Down Shift Layer of Nitrogen-Doped Carbon Quantum Dots (N-CQDs) for Enhanced Current Density and Stability. *Appl. Surf. Sci.* 483, 425–431. doi:10.1016/j.apsusc.2019.03.236

Riaz, S., and Park, S.-J. (2022). Thioacetamide-derived Nitrogen and Sulfur Co-doped Carbon Quantum Dots for "green" Quantum Dot Solar Cells. *J. Industrial Eng. Chem.* 105, 111–120. doi:10.1016/j.jiec.2021.09.009

Roy, P., Chen, P.-C., Periasamy, A. P., Chen, Y.-N., and Chang, H.-T. (2015). Photoluminescent Carbon Nanodots: Synthesis, Physicochemical Properties and Analytical Applications. *Mater. Today* 18, 447–458. doi:10.1016/j.mattod.2015.04.005

Sahoo, S., Satpati, A. K., Sahoo, P. K., and Naik, P. D. (2018). Incorporation of Carbon Quantum Dots for Improvement of Supercapacitor Performance of Nickel Sulfide. *ACS Omega* 3, 17936–17946. doi:10.1021/acsomega.8b01238

Samimi, S., Ardestani, M. S., and Dorkoosh, F. A. (2021). Preparation of Carbon Quantum Dots- Quinic Acid for Drug Delivery of Gemcitabine to Breast Cancer Cells. *J. Drug Deliv. Sci. Technol.* 61, 102287. doi:10.1016/j.jddst.2020.102287

Shah, S. N. A., Zheng, Y., Li, H., and Lin, J.-M. (2016). Chemiluminescence Character of ZnS Quantum Dots with Bisulphite-Hydrogen Peroxide System in Acidic Medium. *J. Phys. Chem. C* 120, 9308–9316. doi:10.1021/acs.jpcc.6b01925

Shejale, K. P., Jaiswal, A., Kumar, A., Saxena, S., and Shukla, S. (2021). Nitrogen Doped Carbon Quantum Dots as Co-active Materials for Highly Efficient Dye Sensitized Solar Cells. *Carbon* 183, 169–175. doi:10.1016/j.carbon.2021.06.090

Shen, J., Zhu, Y., Yang, X., and Li, C. (2012). Graphene Quantum Dots: Emergent Nanolights for Bioimaging, Sensors, Catalysis and Photovoltaic Devices. *Chem. Commun.* 48, 3686–3699. doi:10.1039/C2CC00110A

Shen, P., and Xia, Y. (2014). Synthesis-modification Integration: One-step Fabrication of Boronic Acid Functionalized Carbon Dots for Fluorescent Blood Sugar Sensing. *Anal. Chem.* 86, 5323–5329. doi:10.1021/ac5001338

Shi, Z., and Jayatissa, A. (2018). Perovskites-Based Solar Cells: A Review of Recent Progress, Materials and Processing Methods. *Materials* 11, 729. doi:10.3390/ma11050729

Singh, I., Arora, R., Dhiman, H., and Pahwa, R. (2018). Carbon Quantum Dots: Synthesis, Characterization and Biomedical Applications. *tjps* 15, 219–230. doi:10.4274/tjps.63497

Sk, M. A., Ananthanarayanan, A., Huang, L., Lim, K. H., and Chen, P. (2014). Revealing the Tunable Photoluminescence Properties of Graphene Quantum Dots. *J. Mat. Chem. C* 2, 6954–6960. doi:10.1039/C4TC01191K

Smith, A. M., and Nie, S. (2010). Semiconductor Nanocrystals: Structure, Properties, and Band Gap Engineering. *Acc. Chem. Res.* 43, 190–200. doi:10.1021/ar9001069

Soley, S. S. (2017). "Carbon Quantum Dots : Synthesis and Optronics Applications," in International Conference on Science and Engineering for Sustainable Development, Frankfurt, Germany, February 8–February 10, 2017, 121–124. doi:10.24001/icsesd2017.25

Thambiraj, S., and Shankaran, D. R. (2016). Green Synthesis of Highly Fluorescent Carbon Quantum Dots from Sugarcane Bagasse Pulp. *Appl. Surf. Sci.* 390, 435–443. doi:10.1016/j.apsusc.2016.08.106

Sun, S., Bao, W., Yang, F., Yan, X., Sun, Y., Zhang, G., et al. (2021). Electrochemical Synthesis of FeNx Doped Carbon Quantum Dots for Sensitive Detection of Cu^{2+} Ion. *Green Energy Environ.* doi:10.1016/j.gee.2021.04.005

Sun, T., Zheng, M., Xie, Z., and Jing, X. (2017). Supramolecular Hybrids of Carbon Dots with Doxorubicin: Synthesis, Stability and Cellular Trafficking. *Mat. Chem. Front.* 1, 354–360. doi:10.1039/C6QM00042H

Sun, Y.-P., Zhou, B., Lin, Y., Wang, W., Fernando, K. A. S., Pathak, P., et al. (2006). Quantum-sized Carbon Dots for Bright and Colorful Photoluminescence. *J. Am. Chem. Soc.* 128, 7756–7757. doi:10.1021/ja062677d

Tammina, S. K., Yang, D., Koppala, S., Cheng, C., and Yang, Y. (2019). Highly Photoluminescent N, P Doped Carbon Quantum Dots as a Fluorescent Sensor for the Detection of Dopamine and Temperature. *J. Photochem. Photobiol. B Biol.* 194, 61–70. doi:10.1016/j.jphotobiol.2019.01.004

Tang, D., Liu, J., Yan, X., and Kang, L. (2016). Graphene Oxide Derived Graphene Quantum Dots with Different Photoluminescence Properties and Peroxidase-like Catalytic Activity. *RSC Adv.* 6, 50609–50617. doi:10.1039/C5RA26279H

Tang, X., Yu, H., Bui, B., Wang, L., Xing, C., Wang, S., et al. (2021). Nitrogen-doped Fluorescence Carbon Dots as Multi-Mechanism Detection for Iodide and Curcumin in Biological and Food Samples. *Bioact. Mater.* 6, 1541–1554. doi:10.1016/j.bioactmat.2020.11.006

Teng, P., Xie, J., Long, Y., Huang, X., Zhu, R., Wang, X., et al. (2014). Chemiluminescence Behavior of the Carbon Dots and the Reduced State Carbon Dots. *J. Luminescence* 146, 464–469. doi:10.1016/j.jlumin.2013.09.036

Tian, L., Chen, F., Ding, H., Li, X., and Li, X. (2020). The Influence of Inorganic Electrolyte on the Properties of Carbon Quantum Dots in Electrochemical Exfoliation. *J. Electroanal. Chem.* 878, 114673. doi:10.1016/j.jelechem.2020.114673

Tu, Y., Wang, S., Yuan, X., Wei, Y., Qin, K., Zhang, Q., et al. (2020). A Novel Fluorescent Nitrogen, Phosphorus-Doped Carbon Dots Derived from Ganoderma Lucidum for Bioimaging and High Selective Two Nitrophenols Detection. *Dyes Pigments* 178, 108316. doi:10.1016/j.dyepig.2020.108316

Tungare, K., Bhori, M., Racherla, K. S., and Sawant, S. (2020). Synthesis, Characterization and Biocompatibility Studies of Carbon Quantum Dots from Phoenix Dactylifera. *3 Biotech.* 10, 540. doi:10.1007/s13205-020-02518-5

Tyagi, A., Tripathi, K. M., Singh, N., Choudhary, S., and Gupta, R. K. (2016). Green Synthesis of Carbon Quantum Dots from Lemon Peel Waste: Applications in Sensing and Photocatalysis. *RSC Adv.* 6, 72423–72432. doi:10.1039/c6ra10488f

Unnikrishnan, B., Wu, C.-W., Chen, I.-W. P., Chang, H.-T., Lin, C.-H., and Huang, C.-C. (2016). Carbon Dot-Mediated Synthesis of Manganese Oxide Decorated Graphene Nanosheets for Supercapacitor Application. *ACS Sustain. Chem. Eng.* 4, 3008–3016. doi:10.1021/acssuschemeng.5b01700

Varma, A., Mukasyan, A. S., Rogachev, A. S., and Manukyan, K. V. (2016). Solution Combustion Synthesis of Nanoscale Materials. *Chem. Rev.* 116, 14493–14586. doi:10.1021/acs.chemrev.6b00279

Vercelli, B. (2021). The Role of Carbon Quantum Dots in Organic Photovoltaics: A Short Overview. *Coatings* 11, 232. doi:10.3390/coatings11020232

Wang, B., Wang, S., Wang, Y., Lv, Y., Wu, H., Ma, X., et al. (2016). Highly Fluorescent Carbon Dots for Visible Sensing of Doxorubicin Release Based on Efficient Nanosurface Energy Transfer. *Biotechnol. Lett.* 38, 191–201. doi:10.1007/s10529-015-1965-3

Wang, C., Wu, X., Li, X., Wang, W., Wang, L., Gu, M., et al. (2012). Upconversion Fluorescent Carbon Nanodots Enriched with Nitrogen for Light Harvesting. *J. Mat. Chem.* 22, 15522–15525. doi:10.1039/C2JM30935A

Wang, H.-J., Zhang, J., Liu, Y.-H., Luo, T.-Y., He, X., and Yu, X.-Q. (2017). Hyaluronic Acid-Based Carbon Dots for Efficient Gene Delivery and Cell Imaging. *RSC Adv.* 7, 15613–15624. doi:10.1039/c7ra01417a

Wang, R., Li, G., Dong, Y., Chi, Y., and Chen, G. (2013). Carbon Quantum Dot-Functionalized Aerogels for NO2 Gas Sensing. *Anal. Chem.* 85, 8065–8069. doi:10.1021/ac401880h

Wang, R., Lu, K.-Q., Tang, Z.-R., and Xu, Y.-J. (2017). Recent Progress in Carbon Quantum Dots: Synthesis, Properties and Applications in Photocatalysis. *J. Mat. Chem. A* 5, 3717–3734. doi:10.1039/C6TA08660H

Wang, X., Gao, S., Xu, N., Xu, L., Chen, S., Mei, C., et al. (2021). Facile Synthesis of Phosphorus-nitrogen Doped Carbon Quantum Dots from Cyanobacteria for Bioimaging. *Can. J. Chem. Eng.* 99, 1926–1939. doi:10.1002/cjce.23927

Wang, X., Yang, P., Feng, Q., Meng, T., Wei, J., Xu, C., et al. (2019). Green Preparation of Fluorescent Carbon Quantum Dots from Cyanobacteria for Biological Imaging. *Polymers* 11, 616. doi:10.3390/polym11040616

Wang, Y., Bao, L., Liu, Z., and Pang, D.-W. (2011). Aptamer Biosensor Based on Fluorescence Resonance Energy Transfer from Upconverting Phosphors to Carbon Nanoparticles for Thrombin Detection in Human Plasma. *Anal. Chem.* 83, 8130–8137. doi:10.1021/ac201631b

Wang, Y., and Hu, A. (2014). Carbon Quantum Dots: Synthesis, Properties and Applications. *J. Mat. Chem. C* 2, 6921–6939. doi:10.1039/c4tc00988f

Wang, Y., Kalytchuk, S., Zhang, Y., Shi, H., Kershaw, S. V., and Rogach, A. L. (2014). Thickness-Dependent Full-Color Emission Tunability in a Flexible Carbon Dot Ionogel. *J. Phys. Chem. Lett.* 5, 1412–1420. doi:10.1021/jz5005335

Wang, Y., Yan, L., Ji, G., Wang, C., Gu, H., Luo, Q., et al. (2019). Synthesis of N,S-Doped Carbon Quantum Dots for Use in Organic Solar Cells as the ZnO Modifier to Eliminate the Light-Soaking Effect. *ACS Appl. Mat. Interfaces* 11, 2243–2253. doi:10.1021/acsami.8b17128

Wang, Y., Zhuang, Q., and Ni, Y. (2015). Facile Microwave-Assisted Solid-phase Synthesis of Highly Fluorescent Nitrogen-Sulfur-Codoped Carbon Quantum Dots for Cellular Imaging Applications. *Chem. Eur. J.* 21, 13004–13011. doi:10.1002/chem.201501723

Wen, X., Yu, P., Toh, Y.-R., Ma, X., and Tang, J. (2014). On the Upconversion Fluorescence in Carbon Nanodots and Graphene Quantum Dots. *Chem. Commun.* 50, 4703–4706. doi:10.1039/C4CC01213E

Wu, F., Su, H., Wang, K., Wong, W.-K., and Zhu, X. (2017). Facile Synthesis of N-Rich Carbon Quantum Dots from Porphyrins as Efficient Probes for Bioimaging and Biosensing in Living Cells. *Ijn* Vol. 12, 7375–7391. doi:10.2147/IJN.S147165

Wu, F., Yang, M., Zhang, H., Zhu, S., Zhu, X., and Wang, K. (2018). Facile Synthesis of Sulfur-Doped Carbon Quantum Dots from Vitamin B1 for Highly Selective Detection of Fe3+ Ion. *Opt. Mater.* 77, 258–263. doi:10.1016/j.optmat.2018.01.048

Wu, X., Zhao, B., Zhang, J., Xu, H., Xu, K., and Chen, G. (2019). Photoluminescence and Photodetecting Properties of the Hydrothermally Synthesized Nitrogen-Doped Carbon Quantum Dots. *J. Phys. Chem. C* 123, 25570–25578. doi:10.1021/acs.jpcc.9b06672

Xia, J., Di, J., Li, H., Xu, H., Li, H., and Guo, S. (2016). Ionic Liquid-Induced Strategy for Carbon Quantum dots/BiOX (X = Br, Cl) Hybrid Nanosheets with Superior Visible Light-Driven Photocatalysis. *Appl. Catal. B Environ.* 181, 260–269. doi:10.1016/j.apcatb.2015.07.035

Xu, J., Hou, K., Ju, Z., Ma, C., Wang, W., Wang, C., et al. (2017). Synthesis and Electrochemical Properties of Carbon Dots/Manganese Dioxide (CQDs/MnO2) Nanoflowers for Supercapacitor Applications. *J. Electrochem. Soc.* 164, A430–A437. doi:10.1149/2.1241702jes

Xu, J., Miao, Y., Zheng, J., Yang, Y., and Liu, X. (2018). Ultrahigh Brightness Carbon Dot-Based Blue Electroluminescent LEDs by Host-Guest Energy Transfer Emission Mechanism. *Adv. Opt. Mater.* 6, 1800181. doi:10.1002/adom.201800181

Xu, J., Sahu, S., Cao, L., Bunker, C. E., Peng, G., Liu, Y., et al. (2012). Efficient Fluorescence Quenching in Carbon Dots by Surface-Doped Metals - Disruption of Excited State Redox Processes and Mechanistic Implications. *Langmuir* 28, 16141–16147. doi:10.1021/la302506e

Xu, Y., Liu, J., Gao, C., and Wang, E. (2014). Applications of Carbon Quantum Dots in Electrochemiluminescence: A Mini Review. *Electrochem. Commun.* 48, 151–154. doi:10.1016/j.elecom.2014.08.032

Xu, Z., Liu, J., Wang, K., Yan, B., Hu, S., Ren, X., et al. (2021). Facile Synthesis of N-Doped Carbon Dots for Direct/indirect Detection of Heavy Metal Ions and Cell Imaging. *Environ. Sci. Pollut. Res.* 28, 19878–19889. doi:10.1007/s11356-020-11880-z

Xue, B., Yang, Y., Sun, Y., Fan, J., Li, X., and Zhang, Z. (2019). Photoluminescent Lignin Hybridized Carbon Quantum Dots Composites for Bioimaging Applications. *Int. J. Biol. Macromol.* 122, 954–961. doi:10.1016/j.ijbiomac.2018.11.018

Yan, L., Yang, Y., Ma, C.-Q., Liu, X., Wang, H., and Xu, B. (2016). Synthesis of Carbon Quantum Dots by Chemical Vapor Deposition Approach for Use in Polymer Solar Cell as the Electrode Buffer Layer. *Carbon* 109, 598–607. doi:10.1016/j.carbon.2016.08.058

Yang, J., Jin, X., Cheng, Z., Zhou, H., Gao, L., Jiang, D., et al. (2021). Facile and Green Synthesis of Bifunctional Carbon Dots for Detection of Cu2+ and ClO- in Aqueous Solution. *ACS Sustain. Chem. Eng.* 9, 13206–13214. doi:10.1021/acssuschemeng.1c03868

Yang, S.-T., Cao, L., Luo, P. G., Lu, F., Wang, X., Wang, H., et al. (2009). Carbon Dots for Optical Imaging *In Vivo*. *J. Am. Chem. Soc.* 131, 11308–11309. doi:10.1021/ja904843x

Yang, S., Liang, J., Luo, S., Liu, C., and Tang, Y. (2013). Supersensitive Detection of Chlorinated Phenols by Multiple Amplification Electrochemiluminescence Sensing Based on Carbon Quantum Dots/Graphene. *Anal. Chem.* 85, 7720–7725. doi:10.1021/ac400874h

Yang, S., Sun, J., Li, X., Zhou, W., Wang, Z., He, P., et al. (2014). Large-scale Fabrication of Heavy Doped Carbon Quantum Dots with Tunable-Photoluminescence and Sensitive Fluorescence Detection. *J. Mat. Chem. A* 2, 8660–8667. doi:10.1039/C4TA00860J

Yao, Y.-Y., Gedda, G., Girma, W. M., Yen, C.-L., Ling, Y.-C., and Chang, J.-Y. (2017). Magnetofluorescent Carbon Dots Derived from Crab Shell for Targeted Dual-Modality Bioimaging and Drug Delivery. *ACS Appl. Mat. Interfaces* 9, 13887–13899. doi:10.1021/acsami.7b01599

You, H. R., Park, J. Y., Lee, D. H., Kim, Y., and Choi, J. (2020). Recent Research Progress in Surface Ligand Exchange of PbS Quantum Dots for Solar Cell Application. *Appl. Sci.* 10, 975. doi:10.3390/app10030975

Yu, J., Song, N., Zhang, Y.-K., Zhong, S.-X., Wang, A.-J., and Chen, J. (2015). Green Preparation of Carbon Dots by Jinhua Bergamot for Sensitive and Selective

Fluorescent Detection of Hg2+ and Fe3+. *Sensors Actuators B Chem.* 214, 29–35. doi:10.1016/j.snb.2015.03.006

Yu, Z., Zhang, L., Wang, X., He, D., Suo, H., and Zhao, C. (2020). Fabrication of ZnO/Carbon Quantum Dots Composite Sensor for Detecting NO Gas. *Sensors* 20, 4961. doi:10.3390/s20174961

Zaman, M., Imran, M., Saleem, A., Kamboh, A. H., Arshad, M., Khan, N. A., et al. (2017). Potassium Doped Methylammonium Lead Iodide (MAPbI 3) Thin Films as a Potential Absorber for Perovskite Solar Cells; Structural, Morphological, Electronic and Optoelectric Properties. *Phys. B Condens. Matter* 522, 57–65. doi:10.1016/j.physb.2017.07.067

Zhang, H., Huang, H., Ming, H., Li, H., Zhang, L., Liu, Y., et al. (2012). Carbon Quantum dots/Ag3PO4 Complex Photocatalysts with Enhanced Photocatalytic Activity and Stability under Visible Light. *J. Mat. Chem.* 22, 10501–10506. doi:10.1039/C2JM30703K

Zhang, R., Zhao, M., Wang, Z., Wang, Z., Zhao, B., Miao, Y., et al. (2018). Solution-Processable ZnO/Carbon Quantum Dots Electron Extraction Layer for Highly Efficient Polymer Solar Cells. *ACS Appl. Mat. Interfaces* 10, 4895–4903. doi:10.1021/acsami.7b17969

Zhang, W., Wu, B., Li, Z., Wang, Y., Zhou, J., and Li, Y. (2020). Carbon Quantum Dots as Fluorescence Sensors for Label-free Detection of Folic Acid in Biological Samples. *Spectrochimica Acta Part A Mol. Biomol. Spectrosc.* 229, 117931. doi:10.1016/j.saa.2019.117931

Zhang, W., Zhang, Z., and Zhang, Y. (2011). The Application of Carbon Nanotubes in Target Drug Delivery Systems for Cancer Therapies. *Nanoscale Res. Lett.* 6, 555. doi:10.1186/1556-276X-6-555

Zhang, X., Liu, C., Li, Z., Guo, J., Shen, L., Guo, W., et al. (2017). An Easily Prepared Carbon Quantum Dots and Employment for Inverted Organic Photovoltaic Devices. *Chem. Eng. J.* 315, 621–629. doi:10.1016/j.cej.2017.01.067

Zhang, Y.-Q., Ma, D.-K., Zhang, Y.-G., Chen, W., and Huang, S.-M. (2013). N-doped Carbon Quantum Dots for TiO2-Based Photocatalysts and Dye-Sensitized Solar Cells. *Nano Energy* 2, 545–552. doi:10.1016/j.nanoen.2013.07.010

Zhang, Y., and Wang, T.-H. (2012). Quantum Dot Enabled Molecular Sensing and Diagnostics. *Theranostics* 2, 631–654. doi:10.7150/thno.4308

Zhao, D. L., Das, S., and Chung, T.-S. (2017). Carbon Quantum Dots Grafted Antifouling Membranes for Osmotic Power Generation via Pressure-Retarded Osmosis Process. *Environ. Sci. Technol.* 51, 14016–14023. doi:10.1021/acs.est.7b04190

Zhao, L., Di, F., Wang, D., Guo, L.-H., Yang, Y., Wan, B., et al. (2013). Chemiluminescence of Carbon Dots under Strong Alkaline Solutions: a Novel Insight into Carbon Dot Optical Properties. *Nanoscale* 5, 2655–2658. doi:10.1039/C3NR00358B

Zhao, X., Zhang, J., Shi, L., Xian, M., Dong, C., and Shuang, S. (2017). Folic Acid-Conjugated Carbon Dots as Green Fluorescent Probes Based on Cellular Targeting Imaging for Recognizing Cancer Cells. *RSC Adv.* 7, 42159–42167. doi:10.1039/c7ra07002k

Zheng, J., Zhang, R., Wang, X., and Yu, P. (2019). Importance of Carbon Quantum Dots for Improving the Electrochemical Performance of MoS2@ZnS Composite. *J. Mater Sci.* 54, 13509–13522. doi:10.1007/s10853-019-03860-7

Zheng, X. T., Ananthanarayanan, A., Luo, K. Q., and Chen, P. (2015). Glowing Graphene Quantum Dots and Carbon Dots: Properties, Syntheses, and Biological Applications. *Small* 11, 1620–1636. doi:10.1002/smll.201402648

Zhou, C., Wu, S., Qi, S., Song, W., and Sun, C. (2021). Facile and High-Yield Synthesis of N-Doped Carbon Quantum Dots from Biomass Quinoa Saponin for the Detection of Co2+. *J. Anal. Methods Chem.* 2021, 1–11. doi:10.1155/2021/9732364

Zhou, Q., Yuan, G., Guo, K., Li, S., Lin, M., Hong, J., et al. (2021). Green, Fast and Scalable Preparation of Few-Layers Graphene. *FlatChem* 30, 100303. doi:10.1016/j.flatc.2021.100303

Zhu, H., Wang, X., Li, Y., Wang, Z., Yang, F., and Yang, X. (2009). Microwave Synthesis of Fluorescent Carbon Nanoparticles with Electrochemiluminescence Properties. *Chem. Commun.* 34, 5118–5120. doi:10.1039/B907612C

Zhu, J., Wu, C., Cui, Y., Li, D., Zhang, Y., Xu, J., et al. (2021). Blue-emitting Carbon Quantum Dots: Ultrafast Microwave Synthesis, Purification and Strong Fluorescence in Organic Solvents. *Colloids Surfaces A Physicochem. Eng. Aspects* 623, 126673. doi:10.1016/j.colsurfa.2021.126673

Zhu, S., Song, Y., Zhao, X., Shao, J., Zhang, J., and Yang, B. (2015). The Photoluminescence Mechanism in Carbon Dots (Graphene Quantum Dots, Carbon Nanodots, and Polymer Dots): Current State and Future Perspective. *Nano Res.* 8, 355–381. doi:10.1007/s12274-014-0644-3

Zong, C., Wu, J., Zang, Y., and Ju, H. (2018). Resonance Energy Transfer and Electron-Hole Annihilation Induced Chemiluminescence of Quantum Dots for Amplified Immunoassay. *Chem. Commun.* 54, 11861–11864. doi:10.1039/C8CC06356G

Zong, J., Zhu, Y., Yang, X., Shen, J., and Li, C. (2011). Synthesis of Photoluminescent Carbogenic Dots Using Mesoporous Silica Spheres as Nanoreactors. *Chem. Commun.* 47, 764–766. doi:10.1039/C0CC03092A

Zu, F., Yan, F., Bai, Z., Xu, J., Wang, Y., Huang, Y., et al. (2017). The Quenching of the Fluorescence of Carbon Dots: A Review on Mechanisms and Applications. *Microchim. Acta* 184, 1899–1914. doi:10.1007/s00604-017-2318-9

Zuo, P., Lu, X., Sun, Z., Guo, Y., and He, H. (2016). A Review on Syntheses, Properties, Characterization and Bioanalytical Applications of Fluorescent Carbon Dots. *Microchim. Acta* 183, 519–542. doi:10.1007/s00604-015-1705-3

Conflict of Interest: The authors declare that the research was conducted in the absence of any commercial or financial relationships that could be construed as a potential conflict of interest.

Publisher's Note: All claims expressed in this article are solely those of the authors and do not necessarily represent those of their affiliated organizations, or those of the publisher, the editors, and the reviewers. Any product that may be evaluated in this article, or claim that may be made by its manufacturer, is not guaranteed or endorsed by the publisher.